Graduate School ETD Form 9
(Revised 12/07)

PURDUE UNIVERSITY
GRADUATE SCHOOL
Thesis/Dissertation Acceptance

This is to certify that the thesis/dissertation prepared

By Jeffrey Peter Solzak

Entitled
Molecular and Cellular Mechanisms Leading to Similar Phenotypes in Down and Fetal Alcohol Syndromes

For the degree of Master of Science

Is approved by the final examining committee:

Randall J. Roper
Chair

James A. Marrs

Andrew R. Kusmierczyk

To the best of my knowledge and as understood by the student in the *Research Integrity and Copyright Disclaimer (Graduate School Form 20)*, this thesis/dissertation adheres to the provisions of Purdue University's "Policy on Integrity in Research" and the use of copyrighted material.

Approved by Major Professor(s): Randall J. Roper

Approved by: Simon Atkinson 05/22/2012
Head of the Graduate Program Date

Graduate School Form 20
(Revised 9/10)

PURDUE UNIVERSITY
GRADUATE SCHOOL

Research Integrity and Copyright Disclaimer

Title of Thesis/Dissertation:

Molecular and Cellular Mechanisms Leading to Similar Phenotypes in Down and Fetal Alcohol Syndromes

For the degree of Master of Science

I certify that in the preparation of this thesis, I have observed the provisions of *Purdue University Executive Memorandum No. C-22,* September 6, 1991, *Policy on Integrity in Research.**

Further, I certify that this work is free of plagiarism and all materials appearing in this thesis/dissertation have been properly quoted and attributed.

I certify that all copyrighted material incorporated into this thesis/dissertation is in compliance with the United States' copyright law and that I have received written permission from the copyright owners for my use of their work, which is beyond the scope of the law. I agree to indemnify and save harmless Purdue University from any and all claims that may be asserted or that may arise from any copyright violation.

Jeffrey Peter Solzak

Printed Name and Signature of Candidate

05/22/2012

Date (month/day/year)

*Located at http://www.purdue.edu/policies/pages/teach_res_outreach/c_22.html

MOLECULAR AND CELLULAR MECHANISMS LEADING TO SIMILAR PHENOTYPES IN DOWN AND FETAL ALCOHOL SYNDROMES

A Thesis

Submitted to the Faculty

of

Purdue University

by

Jeffrey Peter Solzak

In Partial Fulfillment of the

Requirements for the Degree

of

Master of Science

August 2012

Purdue University

Indianapolis, Indiana

For my wife.

ACKNOWLEDGMENTS

I would like to thank my family for the enormous amount of support they have given over the years. Without you I would have never been able to do this. I would also like to thank my advisor Randall Roper not only for his teaching capabilities, but for his ability to keep me sane and always being able to put things into perspective.

As for my fellow graduate lab mates, without the two of you this whole experience would have been nowhere near as much fun. Thank you for the laughs on a daily basis!

TABLE OF CONTENTS

Page

Page

LIST OF TABLES

LIST OF FIGURES

ABSTRACT

Solzak, Jeffrey Peter, M.S., Purdue University, August 2012. Molecular and Cellular Mechanisms Leading to Similar Phenotypes in Down and Fetal Alcohol Syndromes. Major Professor: Randall J. Roper.

Down syndrome (DS) and Fetal Alcohol Syndrome (FAS) are two leading causes of birth defects with phenotypes ranging from cognitive impairment to craniofacial abnormalities. While DS originates from the trisomy of human chromosome 21 and FAS from prenatal alcohol consumption, many of the defining characteristics for these two disorders are stunningly similar. A survey of the literature revealed over 20 similar craniofacial and structural deficits in both human and mouse models of DS and FAS. We hypothesized that the similar phenotypes observed are caused by disruptions in common molecular or cellular pathways during development. To test our hypothesis, we examined morphometric, genetic, and cellular phenotypes during development of our DS and FAS mouse models at embryonic days 9.5-10.5. Our preliminary evidence indicates that during early development, dysregulation of *Dyrk1a* and *Rcan1*, cardinal genes affecting craniofacial and neurological precursors of DS, are also dysregulated in embryonic FAS models. Furthermore, Caspase 3 was also found to have similar expression in DS and FAS craniofacial neural crest derived

tissues such as the first branchial arch (BA1) and regions of the brain. This may explain a developmental deficit by means of apoptosis. We have also investigated the expression of pAkt, a protein shown to be affected in FAS models, in cells located within the craniofacial precursor of Ts65Dn. Recent research shows that *Ttc3*, a gene that is triplicated and shown to be overexpressed in the BA1 and neural tube of Ts65Dn, targets pAkt in the nucleus affecting important transcription factors regulating cell cycle and cell survival. While Akt has been shown to play a role in neuronal development, we hypothesize that it also affects similar cellular properties in craniofacial precursors during development. By comparing common genotypes and phenotypes of DS and FAS we may provide common mechanisms to target for potential treatments of both disorders.

One of the least understood phenotypes of DS is their deficient immune system. Many individuals with DS have varying serious illnesses ranging from coeliac disease to respiratory infections that are a direct result of this immunodeficiency. Proteasomes are an integral part of a competent and efficient immune system. It has been observed that mice lacking immunoproteasomes present deficiencies in providing MHC class I peptides, proteins essential in identifying infections. A gene, *Psmg1* (*Dscr2*), triplicated in both humans and in Ts65Dn mice, is known to act as a proteasome assembly chaperone for the 20S proteasome. We hypothesized that a dysregulation in this gene promotes a proteasome assembly aberration, impacting the efficiency of the DS immune

system. To test this hypothesis we performed western blot analysis on specific precursor and processed β-subunits of the 20S proteasome in thymic tissue of adult Ts65Dn. While the β-subunits tested displayed no significant differences between trisomic and euploid mice we have provided further insight to the origins of immunodeficiency in DS.

CHAPTER 1: INTRODUCTION

1.1 Introduction to Down Syndrome and Fetal Alcohol Syndrome

Down syndrome (DS) is the most common genetic disorder that affects approximately 1 out of 750 live births mostly occurring from three copies of chromosome 21 (Hsa21). This chromosomal aberration was first described by Jerome Lejeune in 1959 while conducting research in attempts to cure DS; however many of the distinct phenotypes associated with DS were first defined by John Langdon Down in 1866. DS can occur several different ways with the vast majority (~95%) caused by non-disjunction resulting in a true trisomy (HASSOLD and SHERMAN 2000). Approximately 5% of all other DS cases are caused by Robertsonian translocations, mosaicicm, or partial trisomy of Hsa21. Robertsonian translocations in DS are a result of a hybrid chromosome containing the long arm of Hsa21 and usually the long arm of Hsa14 (BEREND *et al.* 2003). Mosaicisim, the rarest of DS occurrences, is where only a portion of the cells contain a true trisomic nature. These individuals have a tendency to have less severe phenotypes associated with DS and many times go unnoticed.

DS has been defined by over 80 distinct phenotypes that affect craniofacial characteristics, heart, central nervous system, immune system, and

skeletal structure (BLAZEK *et al.* 2011; EPSTEIN 2001; RICHTSMEIER *et al.* 2000; VAN CLEVE and COHEN 2006). Characteristics developing later in life may include immunodeficiency, early onset Alzheimer disease, and celiac disease (EPSTEIN 2001; RAM and CHINEN 2011). Many of these traits however vary widely from individual to individual (WISEMAN *et al.* 2009). Even though the genetic nature of DS has been identified, the mechanisms and pathways that influence these phenotypes are still largely unknown.

Fetal alcohol syndrome (FAS) is a disorder that is caused by the consumption of alcohol by the expectant mother. It affects approximately 1 out of 1000 live births (ABEL and HANNIGAN 1995). This particular disorder has been observed for centuries but it was not until 1973 that two Seattle physicians fully described and brought attention to FAS (JONES and SMITH 1973). Since their publication, concern for FAS has become much more abundant going as far as charging a woman who drank during her pregnancy with felony child abuse in 1991(ARMSTRONG and ABEL 2000).

Many individuals that have FAS present variations of phenotypes as well as severity. This may be due to genetic variation as well as quantity and length of exposure to ethanol during development (ANTHONY *et al.* 2010a; CHEN *et al.* 2011). Many of these phenotypes are much like those found in DS and include craniofacial deficits, abnormalities in neurogenesis, and other structural anomalies (ANTHONY *et al.* 2010a; GRESSENS *et al.* 1992; RILEY *et al.* 2011). Because of the wide range and variation of phenotypes, it is difficult to diagnose

FAS early in life (SCHAEFER and DEERE 2011). These phenotypes arise in development and do not progress in adults. However, due to the damage already done, many individuals with FAS face many behavioral problems and cognitive impairment throughout their lives (FOLTRAN *et al.* 2011; JACOBSON *et al.* 2011; WYPER and RASMUSSEN 2011).

1.2 Mouse models of DS and FAS

Many investigators of DS and FAS use mouse models to emulate traits of these disorders found in humans. While there are several types of mice exhibiting DS like phenotypes, the Ts65Dn mouse model has been most often used with great success. The genes on Hsa21 are mostly conserved in mice; however these genes are separated across three different chromosomes, 10, 16, and 17. Chromosome 16 (Mmu16) in mice contains many of the significant genes, as well as the majority of the DS orthologues found in humans. Ts65Dn contains a trisomic segment of Mmu16 which accounts for approximately half of the gene orthologues that are triplicated in human DS (GARDINER *et al.* 2003). The aneuploidy of this mouse causes similar phenotypes as seen in humans such as reduced mandible and maxillary regions, rostro-caudal dimensions of the neurocranium, and overall reduction and flattening of the face (RICHTSMEIER *et al.* 2000).

FAS investigators have several mouse model resources to study. It has been observed that embryos from different genetic backgrounds vary in

susceptibility to ethanol consumption while also presenting different resultant phenotypes. For this reason, the mouse strain C57BL/6 is the top choice because of its willingness to consume ethanol and the craniofacial features created are the closest to traits found in human FAS (ANTHONY *et al.* 2010a; KHISTI *et al.* 2006; OGAWA *et al.* 2005; SULIK 2005). Investigators also use a culturing method when studying development. Instead of feeding the mother ethanol, the embryos are extracted at a specific time point and placed in an ethanol solution. While culturing embryos may cause differences of expression in specific genes, it is an invaluable way to control the developmental age and amount of ethanol the embryo receives (CHEN *et al.* 2011).

1.3 Phenotypes of DS and FAS

1.3.1 Morphogenic Traits

Anthropometry is the science of measuring the size, weight, or proportions of an organism's body. It has been largely used to compare the differences in humans with DS and FAS to normal individuals as well as the mouse models for these respective syndromes (ANTHONY *et al.* 2010a; RICHTSMEIER *et al.* 2000; RICHTSMEIER and DELEON 2009). Many of these measurements have focused on their defining craniofacial abnormalities. Through measurements using DS and FAS models, investigators found many specific deficits in facial height, width, and depth, as well as smaller orbital regions, nasal length, and ear distances

(ALLANSON *et al.* 1993; ANTHONY *et al.* 2010a; MOORE *et al.* 2002; MOORE *et al.* 2007; RICHTSMEIER *et al.* 2000). Other measurements have concentrated on regions of the brain in which deficits have been observed. Areas such as the hippocampus, cerebellum, and cortex have been shown to be significantly below normal size in both syndromes (CEBOLLA *et al.* 2009; FIDLER and NADEL 2007; LOMOIO *et al.* 2009; NORMAN *et al.* 2009; SERVAIS *et al.* 2007). Using these measurements, regions of interest have been elucidated for molecular and cellular research.

1.3.2 Implications of Neural Crest in Development

The neural crest (NC) is a multipotent stem cell population that emerges and migrates from the neural folds to produce many important tissues throughout development. Once they arrive to their destination, NC can differentiate into a number of different cells. The more specific cranial neural crest (CNC) have the potential to differentiate into cells of the nervous system, bone, and connective tissue (SANTAGATI and RIJLI 2003). The CNC makes up the vast majority of the cell population in the first branchial arch (BA1), a region which gives rise to the mid and lower face including the mandible. For this reason, the BA1 is largely investigated in craniofacial diseases such as DS and FAS. In addition to the mandible, other NC derived structures display deficits as well, including the heart and GI tract (AWAN *et al.* 2004b; BURD *et al.* 2007; HOFER and BURD 2009; WEIJERMAN *et al.* 2010). Ts65Dn mice display NC deficits resulting in craniofacial

and neurological abnormalities (ROPER *et al.* 2009). This NC deficit may be caused by the dysfunction of several integral genes that can be tied to the trisomic nature of DS. In FAS, tissues contain deficits caused by an early and an above normal occurrence of apoptosis where large amounts of NC reside (WANG and BIEBERICH 2010).

1.3.3 Genetic Expression of Cardinal Genes

Of the approximately 300 genes that are triplicated in DS, there are several that have been studied extensively. *Dyrk1a* is a serine-threonine kinase that is found on Hsa21 and is triplicated in most of the major DS mouse models including Ts65Dn. It is an important kinase that regulates many downstream proteins and transcription factors. Some of these transcription factors include cyclic AMP response element-binding protein (CREB), forkhead in rhabdomyosarcoma (FKHR), and nuclear factor of activated T cells (NFAT) (ARRON *et al.* 2006; BRANCHI *et al.* 2004). *Dyrk1a* dysregulation affects many functions such as proliferation, differentiation, and cell survival (YABUT *et al.* 2010). Because of the multiple roles regulated by *Dyrk1a*, it has been implicated in many traits of which neurodegenerative diseases are the most studied (JONES *et al.* 2012; WEGIEL *et al.* 2011a). *Dyrk1a* has been shown to have a role in Alzheimer disease (AD), seen early in DS individuals, by hyperphosphorylating tau causing impaired microtubule assembly and neurofibrillary degeneration (RYOO *et al.* 2008; WEGIEL *et al.* 2011b). The phosphorylation of APP by an

overexpressed *Dyrk1a* is also thought to be a main cause of the pathogenesis of AD (RYOO *et al.* 2008). DS individuals have also presented amyloid senile plaques associated with AD symptoms (PARK *et al.* 2009a). The associated mechanism is an interaction between beta-amyloid precursor protein (APP) and *Dyrk1a* (PARK *et al.* 2007). With APP's location on Hsa21, the expression levels are increased allowing this to occur.

Regulator of calcineurin 1 (*Rcan1* or *Dscr1*) is another gene that has been implicated in several phenotypes in DS. This is done through the increase of Rcan1 and its inhibition of calcineurin, a calcium activated serine/threonine protein phosphatase (FUENTES *et al.* 2000). When calcineurin is inhibited, proteins and transcription factors are not dephosphorylated affecting their activity. *Rcan1* plays several roles and is expressed in many tissues in development including the central nervous system. In adults, *Rcan1* has been shown to be expressed in several tissues such as the heart, liver, and many important regions of the brain including the cerebral cortex and hippocampus (ERMAK *et al.* 2001). It has been implicated in the development of Alzheimer disease by inhibiting the dephosphorylation of tau (LLORET *et al.* 2011). *Rcan1* has also been known to play roles in cardiac and skeletal muscle hypertrophy as well as immunodeficiency through its interaction with Nfat (HARRIS *et al.* 2005; RAM and CHINEN 2011).

Dyrk1a and *Rcan1* have significant interactions with Nfat, an important transcription factor hypothesized to be involved in DS. With a theoretical

increased dosage, both *Dyrk1a* and *Rcan1* may play an inhibitory role on Nfat keeping it from localizing in the nucleus (EPSTEIN 2006). Nfat has been linked to bone development with a role in osteoblast and osteoclast differentiation and homeostasis (ASAGIRI *et al.* 2005; FROMIGUE *et al.* 2010; LEE *et al.* 2009). It also has been investigated as a potential mediator of apoptosis during development, being integral in neurogenesis, and a potential cause of craniofacial abnormalities, cognitive impairment, and motor function (ARRON *et al.* 2006; SRIVASTAVA *et al.* 1999).

1.3.4 Occurrence of Apoptosis

Apoptosis has been a common theme in investigating developmental deficits in individuals with DS and FAS. Although actual mechanisms are still under debate, it has been shown that there is nearly a five-fold increase in apoptosis in the BA1 of embryos treated with ethanol (WANG and BIEBERICH 2010). More specific investigation shows that in developing embryos of several different FAS models, ethanol causes high levels of apoptosis in NC (FLENTKE *et al.* 2011; GARIC-STANKOVIC *et al.* 2005; WANG and BIEBERICH 2010). Other studies show that an epigenetic mechanism, like methylation, may have an effect on pro apoptotic genes in FAS models (LIU *et al.* 2009). Apoptosis has also been studied in DS, however unlike FAS, adult models have had more of a focus. It has been shown that there is a common occurrence of early onset Alzheimer disease accompanied by apoptosis in regions of the brain in individuals with DS

(LU *et al.* 2011). Recent studies confirm an overabundance of apoptosis located in the cerebellum that may be caused by trisomic genes such as *Rcan1* (SUN et al. 2011). Ets2, a gene triplicated in DS, has also been shown to be induced by oxidative stress and has the potential to cause overstimulated proapoptotic pathways in both DS and Alzheimer (HELGUERA *et al.* 2005).Currently there have been studies focusing on apoptosis in DS neural development as well. A recent study found that an increase of S100B, a trisomic gene, may result in apoptosis and oxidative stress in human neural progenitors (LU *et al.* 2011). There have been no investigations to study the possible expression or effects of high occurrence of apoptosis in craniofacial precursors and a possible cause of distinct DS phenotypes.

1.3.5 Expression of Activated Akt in DS and FAS

Understanding the mechanisms behind the craniofacial and neurological deficits of DS remains integral in current research. While *Dyrk1a* and *Rcan1* have been implicated in both facial and neuronal traits, there are many other genes such as *Ets2*, *Olig1*, and *Olig2* that are suspected as well (CHAKRABARTI *et al.* 2010; HELGUERA *et al.* 2005; LU *et al.* 2011). While several genes may play an essential role in the development of these traits, little is known about how much of a role each one has and the underlying pathways involved.

In recent studies, a novel gene that is triplicated in both Ts65Dn and humans with DS that affects neurogenesis when it is expressed at increased

levels has been identified (BERTO *et al.* 2007). This gene, *Ttc3*, is an E3 ligase that targets Akt for ubiquitination when it is activated (SUIZU *et al.* 2009). Akt is a serine/threonine kinase that is responsible for many processes including cell proliferation, cell migration, cell survival, and differentiation (ENOMOTO *et al.* 2005; PENG *et al.* 2003; SHIOJIMA and WALSH 2002; SUIZU *et al.* 2009; WANG and BRATTAIN 2006). It does this by its ability to act on specific transcription factors such as CREB and NF-κB (PATRA *et al.* 2004; WANG and BRATTAIN 2006). For these reasons, it has been highly investigated in several types of cancer as a potential for pharmacotherapy. It has also been observed as a crucial gene in Proteus syndrome, a genetic disorder in which a hyperactive PI3K-Akt pathway causes abnormal bone calcification, overgrowth of skin, brain, connective tissue, and tumor susceptibility (LINDHURST *et al.* 2011). Another protein Akt regulates is p300, a transcriptional coactivatior. When Akt is activated via phosphorylation and is localized in the nucleus, it binds to p300 which then increases histone acetyl transferase activity (HAT) (HUANG and CHEN 2005). With HAT activity increased, transcription factors are able to access DNA that was previously blocked. This also opens DNA access for other proteins such as polymerases to induce transcription.

While pAkt and *Ttc3* have been observed to be dysregulated in DS *in vitro* models, a recent genomic analysis of FAS has shown that Akt is downregulated (HARD *et al.* 2005). Unlike DS, individuals with FAS have decreased inactive form of Akt due to an increase in PTEN, a protein responsible for the inhibition of the

PI3K-Akt cascade (GREEN *et al.* 2007; XU *et al.* 2003). With Akt being profoundly involved in cell survival and the signaling pathway of apoptosis, it is reasonable to assume that apoptosis found in FAS models may be caused by a deficiency of Akt in the BA1.

1.4 Immunodeficiency in Down syndrome

Individuals with DS have been shown for over 30 years to have a decreased functional immune system (BURGIO *et al.* 1978). There are many traits that have been investigated in DS, however, immunodeficiency is one of the least understood. Diseases such as acute lymphoblastic leukemia, hypothyroidism, and coeliac disease are major problems in individuals with DS (BIRGER and IZRAELI 2012; GEORGE *et al.* 1996; SELIKOWITZ 1993). Two of the more abundant problems are respiratory and ear infections. Many of these infections may be caused by morphological traits such as abnormal inner ear canal and tracheomalacia (RAM and CHINEN 2011). While these are thought to be secondary, much of the initial problem lies in the mechanisms that control the immune system. Many of these mechanisms including proteasomal activity, which plays a major role in the immune system, may be regulated by genes that are triplicated in DS.

1.4.1 Proteasomes and immunodeficiency

The 26S eukaryotic proteasome is made up of two sections, a catalytic 20S proteasome and a 19S regulatory particle (SASAKI *et al.* 2010). The 20S proteasome is made up of numerous α and β subunits creating a cylindrical structure. While many recent studies have focused on how this structure is assembled, it is known that there are proteins responsible for helping assemble the proteasomes. One of these helper proteins is called the proteasome assembly chaperone 1 (PAC1). Its responsibility lies in the accurate assembly of the 20S proteasome and in particular dealing with the α subunits. This process using PAC 1 has been shown to be essential in specific tissues of the developing mouse including the brain (SASAKI *et al.* 2010).

Proteasomes are an integral part in sustaining the immune system. They play an important role of removing invading proteins from the cell and slicing them up into pieces via the ubiquitin system. These pieces are then used in creating the peptides used in MHC class I molecule binding. This is the basis for the vertebrate adaptive immunity (KASAHARA *et al.* 2004). There are two major categories of proteasomes, the standard proteasome and the immunoproteasome. The immunoproteasome is the one thought to be specific to create these MHC class I binding peptides (MURATA *et al.* 2008). Within the immunoproteasome category, a more specific proteasome named the thymoproteasome has been discovered recently.

The thymoproteasome is distinct in that the β5 subunit is different from the standard and immunoproteasome. The β5t, the "t" standing for thymus, contains a different configuration in which contains a distinct make-up different than β5i and β5 (FLOREA *et al.* 2010). This difference in composition creates a different peptidase activity compared to other β5 subunits. This type of activity can be characterized by the amino acids present in the S1 pocket of the β5 subunit. Compared to the other two known β5 subunits, β5t contains more hydrophilic residues creating a weaker chymotrypsin-like peptidase activity (MURATA *et al.* 2007). This weaker chymotrypsin-like activity presents a decrease in the Michaelis constant values, however, the overall activity of the proteasome was not changed. It is thought that this difference on protein degrading activity caused by β5t gives rise to specialized peptides, utilized in positive selection of CD8+ T cells (MURATA *et al.* 2008).

1.5 Hypotheses

1.5.1 Similarities in DS and FAS

Individuals with DS and FAS have been observed to present similar morphological phenotypes. For this reason we hypothesize that the Ts65Dn mouse model of DS exhibits analogous craniofacial phenotypes to an FAS mouse model and these phenotypes arise from similar molecular and cellular origin. We examined craniofacial characteristics of our DS and FAS mouse

models by performing microCT scans to confirm previous studies. Molecular comparisons were analyzed by observing the expression of *Dyrk1a* and *Rcan1*, genes of interest in DS, in three embryonic regions of DS and FAS models. We also examined the apoptotic expression in the Ts65Dn at E10 to analyze the patterning as compared to FAS data at similar developmental points. We show that mouse models of DS and FAS exhibit similar molecular and cellular patterns in the craniofacial precursor suggesting a common origin to the abnormal craniofacial development.

1.5.2 pAkt in DS and FAS

The activated form of Akt is exceedingly important in the development of all vertebrates. It is responsible for the regulation of several key transcription factors and proteins involved in an array of cellular processes. Several studies have shown that this protein plays a major role in tissue development, specifically the brain. We hypothesize that pAkt expression is decreased in both DS and FAS in the brain causing neuronal deficits and in the craniofacial precursors resulting in proliferation and cell survival shortfalls. These abnormalities are hypothetically caused by the increased expression of the E3 ligase *Ttc3* in DS and dysregulated PTEN in FAS resulting from ethanol exposure. While both of these syndromes have different origins of how pAkt is affected, the deficits caused by cellular abnormalities will help support the similar craniofacial and neurological abnormalities observed in individuals with DS and FAS.

1.5.3 Proteasome assembly in Ts65Dn

Immunodeficiency is a characteristic in DS that is not well understood. Upon finding a gene that is triplicated in both humans and DS mouse models responsible for proteasome assembly we hypothesize that *Psmg1* (*Dscr2*), a proteasome assembly chaperone, is affected in DS individuals. This dysregulation may cause a decreased number of thymoproteasomes in DS, which can be shown by the levels of precursor versus mature β5t subunits in Ts65Dn. With a decrease in thymoproteasomes, an insufficient library of novel MHC class I binding peptides may be present resulting in the immunodeficiency phenotypes observed in DS.

CHAPTER 2: MATERIALS AND METHODS

2.1 Breeding of mouse model embryos of DS and FAS

Female B6EiC3Sn a/A-Ts(17^{16})65Dn (Ts65Dn), female B6.129S4-Gt(ROSA)26Sor^{tm1Sor}/J (B6.R26R), and C3H/HeJ (C3H) mice were purchased from the Jackson Laboratory (Bar Harbor, ME). B6(R26R)C3F_1 mice were bred by crossing B6.R26R females with C3H males (BLAZEK *et al.* 2011). Ts65Dn E10 embryos were generated by crossing Ts65Dn females with Wnt1-LacZ males. Establishment of embryonic age started at midnight after breeding and plugs were found. E10 embryos were isolated by euthanizing the mother 10 days after plugging.

FAS *in vitro* model embryos were taken at E8 by euthanizing C57BL/6 dams (Harlan, Inc., Indianapolis, IN) with CO_2. The uterus of the dam was placed in 0.1 M PBS at 37º C. Embryos were dissected out of the tissue and placed in PBS containing 4% fetal bovine serum. Three embryos with 3-6 somites were placed into 20 mL culture bottle containing 70% heat-activated rat serum and 30% PB1 buffer. Culture bottles were gassed with air like consistency of 20% O_2, 5% CO_2, and 75% N_2. After preculture period, alcohol exposure consisting of moving the embryos to a medium containing 6 µl/ml of 95% ethanol solution.

Embryos were treated for 44 hours (OGAWA *et al.* 2005). FAS *in vivo* models were generated by treating C57BL/6J dams from E7 to E16 with 4.8% alcohol.

2.2 Polymerase Chain Reaction (PCR) Genotyping

DNA was isolated from toes cut from mice approximately 7-10 days old, born to Ts65Dn dams. Toes were subjected to Proteinase-K (Bioline, Taunton, MA) and T:E:N:S (50 mM Tris pH 7.5, 100mM EDTA pH 8.0, 400 mM NaCl, 0.5% sodium dodecyl sulfate) overnight in a 55º C water bath. Using NaCl, toes were salted out, centrifuged at 13,000 rpm, and precipitated using 95% and 70% ethanol respectively. 50 µl H_2O was added and samples were allowed to remain at room temperature for at least two hours before storage at 4º C.

Original PCR genotyping was performed using gene probes for a single nucleotide polymorphism within the *Zdhhc14* gene on mouse chromosome 17 (Mmu17). Using forward (AAATAGTAGCATCTCATGAGTG) and reverse (GCTTCTCTAAGATGCACTATG) primers (Invitrogen), the triplication could be observed due to DBA/2J allele near the breakpoint of $Mmu17^{16}$ caused by reciprocal translocation from C57BL/6J and C3H/HeJ strains. After PCR, a *Sac I* restriction digest was applied to convert the normal product of 246 bp into two bands of 175 bp and 71 bp. If the trisomic allele was present, the digest would continue to work on normal parental alleles while also showing an uncut 246 bp band. This produced either two bands for positive or one band for negative as the 71 bp band was unable to be seen on agarose gels. This PCR genotyping was

not 100% accurate. FISH was used to confirm Ts65Dn positive pups. (LORENZI *et al.* 2010)

Current PCR genotyping utilizes probes found on either side of Mmu17[16] breakpoint. Probes consisting of Mmu17 forward (GTGGCAAGAGACTCAAATTCAAC) and Mmu16 reverse (TGGCTTATTATTATCAGGGCATTT) were used along with forward (TGTCTGAAGGGCAATGACTG) and reverse (GCTGATCCGTGGCATCTATT) control probes. These two sets of probes provide a 275 bp and 544 bp bands respectively. Ts65Dn positive mice exhibit two bands while negative have one. FISH was not needed to confirm these results. (REINHOLDT *et al.* 2011)

2.3 Fluorescence In Situ Hybridization (FISH) Genotyping

Yolk sacs from embryos were placed in 1.5 mL microcentrifuge tube with 0.5 mL Dulbecco's PBS (DPBS, Mediatech, Inc., Manassas, VA). Collagenase (Type Xl-s, Sigma-Aldrich Corp., St. Louis, MO) was placed into 37º C water bath to thaw and warm. Yolk sacs were centrifuged for 1 minute at 12,000 rpm and the supernatant was removed. They were resuspended in 0.5 mL DPBS, vortexed, and centrifuged again for 1 minute at 12,000 rpm. The supernatant was removed and 0.5 mL of collagenase was added to each tube. They were resuspended and incubated for 30 minutes in the 37º C water bath. The tubes were centrifuged for 1 minute at 12,000 rpm, the supernatant removed, and 0.5 mL 0.075 M KCl was added. They were vortexed and incubated for 30 minutes

more at 37º C. A 3:1 solution of methanol and water was made during the incubation. At the end of the incubation, one drop of the 3:1 fix was added and the tubes were vortexed. They were centrifuged for 1 minute at 12,000 rpm and the supernatant was removed. The pellets were resuspended in 0.5 mL of 3:1 fix making sure that the pellet is dislodged from the bottom of the tube. The samples were stored at 4º C for 24 hours but not more than one week (MOORE *et al.* 1999).

Slides were labeled, creating two slides per sample. Tubes containing samples were centrifuged for 5 minutes at 12,000 rpm and all but 100 µL of 3:1 (methanol:acetic acid) fix was removed. A single drop of distilled H_2O was placed on each slide. The pellet was resuspended with a clean pipet and using the "dropping" technique, the cells were put evenly on each of the two slides. The slides were placed over a beaker of boiling water for approximately one minute to fix the cells, were washed with 3:1 fix, and dried overnight at room temperature.

To hybridize, the slides were incubated for 30 minutes at 37º C in saline-sodium citrate (SSC). At this time, humidified boxes were placed in 37º C incubator to warm and Denhyb (Insistus Biotechnologies, Albuquerque, NM) and probe were allowed to reach room temperature in the dark. Once Denhyb has reached room temperature, it was vortexed and 10:1 Denhyb / probe solution was made allowing for 20 percent more for each slide. The solution was warmed in 37º C water bath. Three coplin jars were filled with 70%, 85%, and 100% ethanol and placed into 4º freezer. The slides were placed into these jars

respectively for two minutes each. The rest of the procedure was done in a darkened room. Two dry baths were warmed to 37º C and 85º C. Each slide was dried and allowed to warm for 3 minutes on 37º C dry bath along with Denhyb / probe solution. Each slide had 7 µL of solution placed on cells, coverslips placed over cells, sealed with rubber cement, and placed on 85º C dry bath for 5 minutes. Slides were placed into preheated humidified box overnight.

For wash and detection of the cells, rubber cement and coverslips were removed and slides were washed in SSC preheated to 68-70º C for 5 minutes. Slides were placed into room temperature SSC for 7 minutes and 8 µL of room temperature Antifade / DAPI (Millipore, Billerica, MA) was placed onto cells. Coverslips were immediately put on and put into slide book. Slides were viewed shortly after for maximum results using a fluorescent microscope. A minimum of 10 cells were counted looking for two or three marker chromosomes showing negative and positive trisomic cells respectively.

2.4 Gene expression analysis of Ts65Dn and Ethanol exposed mouse models

For Ts65Dn embryos, pregnant mothers were euthanized at E10 and the embryos were extracted. Somite age, approximately 24-28 somites, was matched to FAS mouse model counterparts. FISH was performed as previously described on Ts65Dn yolk sac DNA to identify those exhibiting trisomic marker chromosomes. Both embryonic models were dissected into three parts including the head, the BA1, and the remaining body. RNA was isolated from these three

fragments using PureLink RNA micro kit (Life Technologies, Grand Island, NY) and following manufacturer's instructions. RNA was converted to cDNA using Taqman reverse transcription assay reagents (Applied Biosystems, Foster City, CA). Real-Time PCR was performed using target (*Dyrk1a* and *Rcan1*) and endogenous (*Ipo8*) gene probes (Applied Biosystems, Foster City, CA). *Ipo8* was used as the non-dysregulated option for the endogenous gene upon finding out that *Gapdh* was dysregulated in the FAS mouse model. Procedure followed manufacturer's instructions (TaqMan Gene Expression Assay, Applied Biosystems, Foster City, CA)

2.5 MicroCT

Ts65Dn models were anesthetized using isoflurane (Vedco Inc., St. Joseph, MO) in an induction chamber. While sedated, the mice were dissected open, exposing the heart. Using a 25 gauge needle, 40 mL of 4% paraformaldehyde (PFA) was injected into the left ventricle. Immediately after filling the heart to capacity, the right atrium was cut to allow blood to drain. At this time a blood sample was taken for FISH genotyping. All 40 mL was used until the lungs had turned white indicating all of the blood had been replaced. The circulatory system was then flushed with 40 mL of cold 1X PBS. The mice were decapitated and the heads stored in 4% PFA at 4ºC until microCT scan.

FAS embryos were treated with 4.8% ethanol from E7 to E16. FAS scans took place on anethesized mice and was initiated in an induction chamber with

isoflurane levels at 1.5% and 0.8-1.2 liter/min, and maintained at 0.5 liter/min during the 45 minutes scans. Both model scans were performed at postnatal day 21 (p21). All microCT images were acquired with 50 kVp and isotropic 46 µm resolution using EVS-R9 system (GE Healthcare, Waukesha, WI) at the Indiana University School of Medicine.

2.6 Immunohistochemistry

Both DS and FAS embryo models, once cultivated, were placed in 4% PFA for a minimum of 2 days. One experimental and control embryo were placed in a 10% gelatin mold which was allowed to harden at and placed in 4% PFA at 4º C for a minimum 2 days. These molds were then trimmed and sectioned on a vibratome (Leica Biosystems Inc., Richmond, IL) at 40 µm. Sections were placed in a vial with 0.1 M PBS for storage. The sections were washed initially with 0.1 M PBS and treated for 10 minutes in 3% H_2O_2. Once washed again in PBS, they were exposed to 1% Triton X-100 overnight. The next day, the sections were washed again and blocked in Goat kit buffer (0.1% Triton X-100 and 1.5% normal goat serum in 0.1 M PBS) for 90 minutes on a shaker. Cleaved caspase-3 (Cell Signaling Technology, Boston, MA) was used as a primary antibody at 1:150 dilution and incubated overnight. Washed again in PBS, the sections were incubated for 90 minutes in biotin conjugated goat anti-rabbit secondary antibody at 1:500 dilution (Jackson ImmunoResearch, West Grove, PA). Yet another wash in PBS, the sections were then incubated for another 90 minutes in peroxidase-

conjugated streptavidin using 1:500 dilution (Jackson ImmunoResearch, West Grove, PA). The sections were then washed in PBS six times and in 0.05M TBS four times. Incubation of the sections was done in 0.05% Diaminobenzidine (DAB, Sigma-Aldrich, St. Louis, MO) in 0.05 M TBS with an additional 10-15 minutes of 0.003% H_2O_2 added. Sections were washed four times in 0.05M TBS and six times in 0.1 M PBS. Once the sections were placed on slides, they were dried overnight. They were Nissl counterstained with methyl green to show contrast of the c-caspase-3 stain (CHEN *et al.* 2011).

2.7 Protein Homogenization from adult tissue

Homogenization buffer was created using 150 mM NaCl, 20 mM Tris-HCl, 0.2% NP40, 1.0% protease inhibiting cocktail, and Millipore water added to 10 mL. The buffer solution was chilled by placing on ice for >10 minutes. To homogenize, appropriate sized tissue was placed in labeled 1.5 mL centrifuge tubes. 400 mL of cold homogenization buffer was placed into the tubes containing the tissue and promptly homogenized with a motorized mortar and pestle. Tissue was spun in centrifuge for 15 minutes, 13,000 rpm, and 4º C. Being careful to not take pellet at the bottom or the lipid layer at the top, 200 mL was taken out of spun homogenization. The protein solution was put into another tube and spun again for 10 minutes under same conditions. In the same fashion 100 mL was taken out, placed into new tubes, and was immediately placed on ice.

2.8 BCA protein concentration assay

Protein concentration was evaluated using the Bicinchoninic acid (BCA) technique. The assay solution used was made up of BCA solution A and Solution B (ThermoFisher Scientific, Waltham, MA) at 50:1 respectively. All samples tested had 1.0 mL added to each cuvette. For controls; 35.0, 42.5, 46.2, and 48.1 µL of homogenization buffer was added to samples with 50 µL of buffer added to blank. To those controls; 15, 7.5, 3.75, and 1.88 µL of BSA protein was added respectively to samples to have a total of 50 µL of sample with the assay solution. For each tissue sample, 5 µl was added to 45 µL of homogenization buffer along with the 1.0 mL of assay solution in each cuvette. The control samples were then placed into the spectrometer (BioMate 3S, ThermoFisher Scientific, Waltham, MA) and absorbance was measured at 562 nm. The tissue samples were then placed and measured in the same fashion. Using the absorbance and µg of BSA protein in each solution, a graph was created. Using line of best fit and creating an equation using Microsoft Excel, tissue sample protein concentration was formulated. The amount of µg in each sample was divided by 5 to get a final number of µg/µL. Samples for loading were created based upon these final numbers. 20 µg of protein was calculated and added to Millipore H_2O to have a final volume of 20 µL. To the protein and H_2O, 4 µL of 5x Laemmli loading buffer was added. The samples were boiled for three minutes, allowed to cool, and loaded into polyacrylamide gels.

2.9 Polyacrylamide Gel Electrophoresis

Loading plates were cleaned as to be sure that there was no dirt or dust that would ruin the gel. The 1.0 mm plates were placed into the holder for loading of the gels. Two gels were used, a 12% running gel and a 4% stacking gel. 5mL of running gel was created using 1.41 mL diH_2O, 1.25 mL resolving buffer (1.5 M Tris-HCl pH 8.8), 1.46 mL 40% polyacrylamide (Bio-Rad Laboratories, Inc. Hercules, CA), 0.8 mL bisacrylamide (Bis) (Bio-Rad Laboratories, Inc.), 25 µL 20% SDS (Sigma-Aldrich, St. Louis, MO), 5 µL Tetramethlyethylenediamine (TEMED, Sigma-Aldrich), and 50 µL 10% Ammonium Persulfate (APS, Sigma-Aldrich) was added when gel was ready to load into plates. The solution was added to the plates to approximately 1.0 cm below the top of the plates. Immediately isopropanol was added to ensure that the top of the gel was covered. While the gel is setting, the stacking gel was created using 1.74 mL diH_2O, 312.5 µL 8x stacking buffer (1 M Tris-HCl pH 6.8), 241.5 µL polyacrylamide, 166.5 µL Bis, 12.5 µL 20%SDS, 2.5 µL TEMED, and 25 µL of 10% APS when gel is ready to be loaded. Once the running buffer was set, the isopropanol was absorbed using filter paper, rinsed with water and absorbed with filter paper again. The stacking buffer was loaded into the plates to the top and the 1.0 mm comb for the gel was placed into the plates, ensuring that there are no bubbles. Once the gel has been set, approximately 10-15 minutes, the comb was removed and the wells of the gel rinsed with distilled water. The gel was

placed into the gel apparatus and running buffer was filled to the designated line according to manufacturer's directions (Bio-Rad Laboratories, Hercules, CA). Each PAGE was run at 80 volts (v), 400 milliamps for 20-30 minutes until protein has migrated past the stacking gel. The voltage was increased to 120 v for approximately 1-1.5 hours until dye migrated out of the gel.

2.10 Western Blot

The SDS-PAGE gel was taken out of the gel apparatus and soaked in trans-buffer solution. Six pieces of filter paper, three for each side, was cut to the size of the gel. PVDF membrane was also cut to the same size. The PVDF was soaked in methanol to ensure absorption of tris-glycine transfer buffer. The PVDF was taken out of the methanol and soaked in tris-glycine buffer. The filter paper was placed in the tris-glycine buffer as well. A sandwich was created with three pieces of filter paper on the bottom, the PVDF membrane next, the SDS-PAGE gel, and then the final three pieces of filter paper. This sandwich was placed in a Bio-Rad Transfer cell with the PVDF membrane below the SDS-PAGE gel. The power source was run at 15 v, 0.9 A, and 30 W for a duration of 25 minutes. The transfer was found to be successful if the bands from the ladder were seen on the PVDF membrane.

In a tray, the PVDF membrane was soaked in a 1X TBS solution to rinse the salts for five minutes. The TBS was poured off and 10 mL of 5% (w/v) non-fat milk powder solution in 1X TBS was poured over the membrane. This was

allowed to block the membrane overnight at 4º C. After incubation, the blocking buffer was poured off and primary was added at 1:1000 dilution for β5t antibody (Enzo Life Sciences, Inc., Farmingdale, NY) and was incubated at room temperature for 60 minutes. The membrane was then washed three times for five minutes each in 1X TBS with 0.1% Tween 20 (Sigma-Aldrich, St. Louis, MO).The secondary was added using TBS-Tween at a dilution of 1:4000 and was incubated for another hour at room temperature. The membrane was washed again another three times for five minutes using TBS-Tween.

For exposure, the membrane was taken out of the wash and placed into new tray. The detection solution, 1.0 mL, was added to the membrane for 1.5-2 minutes ensuring that the whole membrane was covered. The solution was then allowed to run off and the membrane was placed into a sleeve making sure no bubbles were present. This was then taped into the film cassette and exposed in the dark room for 30 seconds, 45 seconds, one minute, and two minutes. Film was then developed and scanned for analysis.

2.11 Cryostat embedding and sectioning

Embryos were dissected from Ts65Dn positive dams and yolk sac DNA was isolated for genotyping. Embryos were fixed in 4% paraformaldehyde, 5% sucrose in 0.1M phosphate buffer (pH 7.4) for 90 minutes. Embryos were rinsed in 1X PBS two times for 10 minutes. Infiltration of the embryos was allowed to take place overnight in 20% sucrose in 0.1 M phosphate buffer.

Before embedding a 3:1 mixture of the 20% phosphate buffer solution and Tissue-Tek OCT embedding compound (Sakura Finetek USA, Inc., Torrance, CA) was allowed to sit for 20 minutes while dry ice was obtained. Molds were filled halfway with OCT mixture, placed into tray with a dry ice-70% EtOH mixture, and embryos were oriented using a dissecting microscope. The mold was then filled and allowed to freeze in the dry ice. Embryo molds were stored at -80º C. Before cryostat sectioning, molds were placed into -20º C freezer for one hour.

2.12 Immunofluorescence

The slides were removed from -80º C freezer and allowed to come to room temperature. The slides were washed in 1X PBS for 10 minutes. For permeablization, slides were washed with gentle shaking in 1X PBS with 0.5% Triton X-100 for 15 minutes. They were then exposed to antigen retrieval in 1X PBS with 1% SDS for 5 minutes. The slides were washed in 1X PBS with 0.2%Triton X-100 three times for 5 minutes making sure all SDS was removed. Sections on the slides were circled with PAP pen to create a hydrophobic barrier and promptly placed into humidified chamber for 20 minutes to prevent sections from drying out. Tissues were blocked with goat blocking buffer (5% normal goat serum, 0.025% Triton X-100, in 1X PBS) for 60 minutes at room temperature. The blocking buffer was carefully removed and primary antibody for pAkt (Cell Signaling) was added, 1:200 dilution factor in blocking buffer, and placed in

humidified chamber at 4º C overnight. The next day the slides were taken out of the fridge and allowed to come to room temperature. Excess antibody was carefully removed and slides were washed two times for 10 minutes in 1X PBS with 0.2% Triton X-100 at room temperature. In a dark room, the appropriate Alexa-fluor secondary antibody (Invitrogen) was applied at 1:1000 dilution in PBS with 0.2% Triton X-100 and incubated for 60 minutes. Excess antibody was removed and slides were washed 10 minutes each in PBS Triton X-100 and PBS. Pro gold Dapi/Antifade (Life Technologies, Grand Island, NY) mounting media was added and coverslips were applied. Each side of the coverslip was sealed using clear nail polish and allowed to dry. Slides were stored at 4º C in the dark until pictures could be taken using Olympus FV-111-MPE confocal multiphoton microscope (Olympus, Center Valley, PA).

2.13 Immunofluorescence Analysis

Comparison of tissues was performed by using similar embryonic cross sections which were found by observing tissues present in each section. After immunostaining, using the sections, tissues were qualitatively analyzed for differences. This was performed by utilizing ImageJ (National Institute of Health, Bethesda, MD). The pAkt image had the background intensity subtracted by using the Math function. The amount of background that was subtracted stayed the same throughout all pictures, 200, to restrict any bias. The nuclei picture was then selected and threshold was established. Once again, the threshold number

remained the same, 500, throughout the analysis to restrict bias. The nuclei picture was then divided by the value of 255 to remove any background. Using the image calculator, the pAkt image was multiplied by the nuclei picture giving fluorescent expression only in the nucleus. Using the measuring tool, the mean intensity was gathered from the multiplied picture and the pAkt picture. The final step was to divide the fluorescence found in the nuclei by the total found for pAkt. This number gave the percent fluorescence in the nuclei alone. After the analysis was complete, a summary was produced. The fluorescence value and standard deviations were recorded and plotted in Excel.

CHAPTER 3: RESULTS

3.1 Craniofacial analysis of DS and FAS

Because craniofacial deficits are observed in both DS and FAS, we examined previously published literature to identify precise anthropometric measurements for comparison. Approximately twenty craniofacial measurements, including facial depth, canthal distances, nasal length, and maxillary and mandibular arc, were found that corresponded to DS and FAS in both human and mouse models (Table 1). All of the measurements were observed to be similar with only one measurement, the minimal frontal breadth, differing between DS and FAS mouse models. With the tremendous amount of similarity of craniofacial measurements, other physiological traits were investigated including the brain, heart, and other organs and structures. The brain presented many of the same deficits in both DS and FAS including an abnormal dentate gyrus in the hippocampus, reduced number of Purkinje cells in the cerebellum, reduction of cerebellar size, and overall neuronal impairment of the cortex. The heart, kidneys and gastrointestinal (GI) tract all displayed similar morphological irregularities including septal defects in the heart and pseudoobstructions of the GI tract. Observing similarities in over 30 unique measurements and characteristics between DS and FAS, we hypothesized that

Ts65Dn and ethanol treated FAS mice would also display these similar characteristics. To achieve this, microCT scans using DS and FAS models at P21 were performed. Using nine corresponding craniofacial dimensions from previous studies (ANTHONY *et al.* 2010a; RICHTSMEIER *et al.* 2000), we confirmed at P21, these craniofacial characteristics are similarly abnormal in DS and FAS mouse models at P21. Nine measurements including minimal frontal breadth, inner orbital width, facial depth, nasal length, and bitragal width were all chosen as representations of phenotypes observed in humans with DS and FAS (Figure 1). These skeletal differences show deficits in cranial size, eye size and separation, as well as flattening of the face that leads to secondary traits such as breathing and feeding problems (RESTA *et al.* 2003; SPENDER *et al.* 1996).

3.2 Altered *Dyrk1a* and *Rcan1* expression in DS and FAS embryos

The BA1 is the developmental precursor to the mid and lower face which includes the mandible and maxillary region. This area includes many of the craniofacial abnormalities observed, including a reduced mandible, in both DS and FAS. *Dyrk1a* and *Rcan1*, genes triplicated in both humans with DS and Ts65Dn mice, are thought to be partially responsible for numerous traits in DS including neurological deficits as well as craniofacial and bone abnormalities (ARRON *et al.* 2006; DEITZ and ROPER 2011; PARK *et al.* 2009b). With *Dyrk1a* and *Rcan1* dysregulation found in DS models, both in development and in adults, we

hypothesized that there would also be a dysregulation of these cardinal genes in FAS embryos.

Testing three different tissues, BA1, head, and the remainder of the body, we observed many irregularities. The BA1, being the most specific structure we tested, displayed the most consistent similarities between DS and FAS and had significant fold changes of *Dyrk1a*. In Ts65Dn at E10, *Dyrk1a* expression was significantly decreased by 0.644 fold average as compared to euploid littermates. This was similar to our findings in FAS where *Dyrk1a* expression was decreased by 0.701 fold change (Figure 2). *Rcan1* in our DS and FAS models were both upregulated. Ts65Dn displayed a fold change increase of 1.26, while the ethanol treated embryos had a fold change increase of 1.96 (Figure 3).

Performing qPCR analysis on the head of DS and FAS mouse models also displayed dysregulation of these key genes, however, they were not similar in expression. Ts65Dn head exhibited a decreased expression of *Dyrk1a* (0.605) while displaying and increase of *Rcan1* (1.244) as compared to euploid littermates. The ethanol treated FAS model had a small increase of *Dyrk1a* (1.098) and a decreased expression of *Rcan1* (0.807). Within the bodies of DS and FAS mice differences in expression were also present. *Dyrk1a* had a fold change decrease of 0.675 in Ts65Dn while displayed no significant change in *Rcan1* expression. The ethanol treated embryos presented an increased fold change of *Dyrk1a* (1.377) and a small increase of *Rcan1* (1.126) (Table 2).

3.3 Analysis of apoptosis using c-Caspase 3 in the BA1 and the brain

Ethanol induced apoptosis has been studied extensively in FAS as a cause of craniofacial and neurological phenotypes (CARTWRIGHT and SMITH 1995; SU *et al.* 2001; SULIK 2005). For this reason, to fully understand the comparison between DS and FAS, we examined apoptotic patterning at a similar developmental stage. Embryos of both models were taken at approximately E10 and somite matched at approximately 24-28 somites. Cells undergoing apoptosis in these embryos were observed through immunohistochemistry using an antibody for cleaved caspase 3 (c-caspase 3). The patterning that resulted displayed expression of the activated caspase 3 in both control and trisomic embryos within the BA1 and three regions of the brain; the forebrain, midbrain, and hindbrain (Figure 4). These regions of the embryos were quantified carefully by counting the amount of cells with caspase 3 expression present. The resulting numbers were expressed as a ratio of c-caspase 3 cells in trisomic tissue versus euploid tissue. The four trisomic regions, the BA1, forebrain, midbrain, and hindbrain, contained increases of 2.36:1, 2.67:1, 1.51:1, and 1.20:1 respectively (Table 3). FAS embryo models also contained increases within the BA1, forebrain, midbrain, and hindbrain of 5.47:1, 3.29:1, 2.52:1, and 1.59:1 respectively. The FAS models have a more significant increase, however both models to present a modest increase in apoptosis compared to their respective controls.

3.4 Increased expression of *Ttc3* causes a decrease in pAkt

To test our hypothesis that *Ttc3* is in fact overexpressed and pAkt levels are decreased *in vivo* within craniofacial precursors, we used Ts65Dn E9.5-E10.5 head, neural tube (NT), and BA1. Performing qPCR using *Ttc3* probes, the expression levels were tested in the three tissues. It was observed that in the head, E10.5 Ts65Dn heads displayed a 1.486 fold change when compared to control heads. In E9.5 Ts65Dn embryos, the NT and BA1 displayed an increase of 1.443 and 1.413 respectively compared to control embryos (Figure 5). These fold changes were theoretically expected due to the trisomic nature of *Ttc3*.

Knowing that our DS mice models contained an increased expression of the pAkt E3 ligase in development, we used immunofluorescence to test the levels of pAkt in the BA1. Embryos were taken at E9.5 and sectioned. After staining, sections were matched as closely as possible to ensure similar tissue sections were compared. Through initial qualitative analysis, it was observed that within the nucleus there was a much higher expression of pAkt in control sections when compared to our trisomic embryos (Figure 6, 7). It was also observed that the number of cells in the trisomic BA1 was decreased and that there seems to be a lack of organization of those cells.

The intensity of the localization of pAkt in the nucleus was quantified using ImageJ. Testing sections of seven embryos, four trisomic and three euploid, the fluorescence percentage for pAkt in the nucleus at 80X was determined. It was found that the percent fluorescence of pAkt in trisomic nuclei

was approximately 24.435% with 57.324% fluorescence found in euploid nuclei (Figure 8). This quantification supports the qualitative analysis by showing a significant increase in percent of pAkt in control BA1 nuclei *in vivo* compared to trisomic BA1 nuclei.

3.5 β5t and β6 protein levels in Ts65Dn thymus

Immunodeficiency in DS mouse models may be caused by a dysregulation of the assembly of the 20S proteasome in the thymus. This dysregulation irregularity may be caused by the proteasome assembly chaperone, *Psmg1* (*Dscr2*), which is triplicated in both Ts65Dn and in humans with DS. To observe this this potential aberration of 20S proteasome assembly, the thymus and brains of trisomic and euploid mice of similar ages, 8-12 weeks, were extracted for protein isolation. With the protein isolated, western blots were performed using β5t and β6 antibodies to observe any differences. β6, and more importantly β5t, are subunits integral in the structure of the thymoproteasome. We performed western blots on tissue from the Ts65Dn thymus to indicate any irregularities in the thymoproteasome as a potential cause of immunodeficiency as well as on the brain which served as control tissue. Our results show that while there is a small difference in protein levels of both processed and precursor β5t and β6 subunits, that these levels were likely not significant enough to cause the immunodeficiency observed in our DS mice (Figure 9).

CHAPTER 4: DISCUSSION

4.1 DS and FAS Craniofacial Analysis

Our first observation that individuals with DS and FAS had similar facial features led us to examine previous anthropometric literature. Traits such as reduced mandible, overall midface hypoplasia, and almond shaped eyes are among those distinct in individuals with and mouse models of DS (ALLANSON *et al.* 1993; RICHTSMEIER *et al.* 2000). Similar studies of craniofacial traits in individuals and mouse models of FAS displayed many of the same craniofacial abnormalities (ANTHONY *et al.* 2010a; MOORE *et al.* 2002; MOORE *et al.* 2007). Our hypothesis that these two syndromes are similar is based upon the cells that create and develop many of these craniofacial traits originate from the same region, the neural crest.

While these studies were important for the initial investigation of the comparison between DS and FAS, it was necessary to compare both our respective mouse models at similar developmental ages to ensure no bias. MicroCT analysis of both models at P21 demonstrated and confirmed similar craniofacial deficits as seen in humans. Furthermore, the minimal frontal breadth that was observed to be dissimilar in previous DS and FAS studies was found to present the similar deficit in our models. This discrepancy is most likely caused

by the difference in the age of the mice that was originally measured in the previous studies. This was certainly corrected by the comparison at a similar developmental age.

While the genetic background of these two mouse models may be fundamentally different, we feel that it only supports our hypothesis that two different syndromes can present similar phenotypes that occur through similar cellular and molecular pathways. Ts65Dn, with the specific background of B6(R26R)C3F_1 and Ts65Dn, have been used for years as one of the standards in DS studies. It is this background that makes this mouse model the one that most closely emulates phenotypes that are seen in humans with DS. FAS investigators also have several genetic backgrounds of mice that serve as good models, however, the model C57BL/6 is one that freely consumes alcohol while also presenting many of the same physical and cognitive traits as humans with FAS. As we and previous studies have shown, DS and FAS display extremely similar morphological traits not only in their respective mouse models, but also in humans.

4.2 Cardinal Genes *Dyrk1a* and *Rcan1*

Dyrk1a and *Rcan1* have both been integral in understanding many of the phenotypes associated with DS. These two genes are closely tied to phenotypes ranging from craniofacial deficits to the occurrence of early onset Alzheimer disease. Both *Dyrk1a* and *Rcan1* are able to regulate specific proteins and

transcription factors such as Nfat and CREB making the dysregulation of these genes detrimental (KIM and SEO 2011; PARK *et al.* 2009a). *Rcan1* has also been studied in more specific mechanisms such as its effects on apoptosis in DS brains via caspase 9 and caspase 3 activation. *Dyrk1a* has displayed many cellular roles such as development of the brain, effects on cell survival, craniofacial abnormalities. For these reasons, it was important to examine the expression of these key genes in and FAS system model.

Our qPCR analysis of *Dyrk1a* and *Rcan1* exhibited a dysregulation in all three tissues; BA1, head, and body, in both Ts65Dn and ethanol treated embryos at E10.5. Similarities in genetic expression within the BA1 of both of our DS and FAS models were the most significant with its role in craniofacial development. At this developmental age, *Dyrk1a* was decreased similarly and *Rcan1* was increased in both DS and FAS models. In the head and the body, both of these genes were dysregulated but differently from one another. One explanation of this anomaly is that the tissue encompassed too general of an area. The BA1 is a specific structure with a smaller population of cells that are derived from the same source, whereas the head and the body are derived from several different populations of cells.

Dyrk1a and *Rcan1*, two genes that are integral in development, are dysregulated in both DS and FAS mouse models. Many investigators hypothesize that these two genes are possibly dysregulated in DS due to their triplication in DS models, but for the first time we have shown that prenatal

exposure to ethanol has an effect on their expression. This dysregulation of *Dyrk1a* and *Rcan1* can help explain the similarities in craniofacial and cognitive phenotypes in both DS and FAS and may provide future targets for the treatment of these two syndromes.

4.3 Occurrence of Apoptosis in DS and FAS

An increased incidence of cell death that occurs naturally in development has been well documented in FAS. It has been previously reported that prenatal exposure to alcohol causes apoptosis in NC derived tissues such as the BA1 as well as the brain and cranial nerves (DUNTY *et al.* 2002; WANG and BIEBERICH 2010). In Ts65Dn, it has been observed that there is a proliferation and migration deficit in the NC (ROPER *et al.* 2009). We aimed to show that not only are there proliferation and migration deficits in Ts65Dn, but there is also an overabundance of apoptosis in tissue critical for development, similar to observations in FAS models. Here we show that in the Ts65Dn BA1 that there is over two-fold more c-caspase 3 expression than in the controls. This cleaved form of caspase 3, known as an excecutioner caspase, is present when there is apoptosis occurring in cells. This two-fold increase is similar to ethanol treated embryos that displayed an approximately five-fold increase in the same tissue. It is important to note that while there was a much higher level of apoptosis occurring within the ethanol treated embryos, possibly from the culturing methods itself, it was still greater than the cultured controls they were compared to.

In the brain, there is approximately 1.5-2 fold increase of c-caspase 3 in the frontal, mid, and hindbrain of the Ts65Dn embryos. This data shows that an increase in normal apoptosis may be a cause of cognitive impairment we observe in individuals with DS. It has been previously described that apoptosis is present in human neural progenitor cells found in ventricular and subventricular zones of the cortex and in the frontal cortex of early postnatal Ts65Dn mice (LU *et al.* 2011). Our data, however, for the first time shows an increase of apoptosis occurs early in development in Ts65Dn. This deficit found in our DS model emulates the apoptotic patterning found in ethanol treated embryos (CHEN *et al.* 2011; SARI 2009).

While proliferation and migration deficits are seen within the NC of Ts65Dn, it is important to show that an overabundance of apoptosis the DS mouse model may also cause abnormalities. Both DS and FAS models have now been shown to present above normal apoptotic expression during development not only in the brain, but also in the BA1 which is attributed to craniofacial precursors. Along with the genetic expression of *Dyrk1a* and *Rcan1*, similar aberrant expression of apoptosis in development is an important step in comparing the distinct phenotypes we observe in both DS and FAS mouse models.

4.4 pAkt expression in Ts65Dn

A previous study observed that an E3 ligase, *Ttc3*, effectively degrades the protein Akt while in its active form in the nucleus. This pAkt mechanism regulates transcription factors such as CREB and Foxos, having effects on cell survival, proliferation, and differentiation. It also has been shown to affect other proteins such as transcriptional coactivatior p300, thus affecting the transcriptional potential of many genes (HUANG and CHEN 2005). *Ttc3* is triplicated both in Ts65Dn and in humans. We have shown here that the genetic expression at E9.5-E10.5 in Ts65Dn BA1, NT, and head is in fact increased approximately 1.5 times euploid levels. With an increased expression of Ttc3 found in Ts65Dn and its potential effect on pAkt levels, we investigated and observed a decrease in pAkt within the nucleus of cells located in the BA1.

An increase of the oncoprotein Akt has been shown to induce overgrowth in craniofacial, brain, and other tissues as observed in Proteus syndrome where this overgrowth is a major phenotype (LINDHURST *et al.* 2011). Our hypothesis states that a decrease of pAkt would hinder growth and decrease cell survival within the craniofacial precursors in Ts65Dn embryos. While further studies must be shown to investigate the actual effects of pAkt on cells in the BA1, the observed decrease of pAkt is a positive step in explaining some of the deficits in the BA1 at E9.5-E10.5.

The decreased pAkt seen in Ts65Dn also corresponds to an Akt deficit seen in FAS rat models caused by an increase in the phosphatase PTEN (GREEN

et al. 2007; Xu *et al.* 2003). While the origin of the observed deficit of activated Akt in DS and FAS is dissimilar, the outcome is the same. This phenomenon also explains the increase in apoptosis that we observe in both models with one of Akt's primary roles being cell survival.

4.5 Immunodeficiency in DS

Over several decades, the origin of the immunodeficiency in DS has been examined. Several distinct illnesses such as coeliac disease and lymphoblastic leukemia have an increased presence in those with DS. Many of these illnesses are secondary in nature occurring from structural abnormalities such as heart and gastrointestinal defects. Even with the cause of some of these illnesses being caused by structural deficits, the underlying problem is located within the immune system.

A gene, *Psmg1* (*Dscr2*), is triplicated in individuals with DS and is responsible for aiding the assembly of proteasomes. The potential dysregulation of the proteasome machinery presents a major problem in the immune system. *Psmg1* plays a role in processing subunits that make up the proteasome. The subunits that are processed irregularly may cause a deficient immune system. To observe this, we investigated the processed levels of the β5t subunit, a major part of the 20S thymoproteasome. Observing the levels of both the precursor and processed β5t protein within the thymus of Ts65Dn, we found no significant difference compared to euploid mice. Although the gene responsible for the

assembly of the 20S proteasome contains three copies, it seems to have no effect on this facet of the immune system.

Many new studies on immunodeficiency in DS have focused on other factors within the immune system such as decreased naïve T cell numbers. Naïve T cells are an important part of the immune system, playing a role in identifying newly acquired pathogens that have not been present before. A recent study has shown that the low numbers of these T cells is caused by a decreased thymic output (BLOEMERS *et al.* 2011). While more studies have focused on the decreased levels of naïve T cells and overall thymic output, for the first time we report that there is no significant complication with proteasome assembly that would support the observed immunodeficiency in DS.

REFERENCES

REFERENCES

Abel, E. L., and J. H. Hannigan, 1995 Maternal risk factors in fetal alcohol syndrome: provocative and permissive influences. Neurotoxicol Teratol **17:** 445-462.

Allanson, J. E., P. O'Hara, L. G. Farkas and R. C. Nair, 1993 Anthropometric craniofacial pattern profiles in Down syndrome. Am J Med Genet **47:** 748-752.

Anthony, B., S. Vinci-Booher, L. Wetherill, R. Ward, C. Goodlett *et al.*, 2010a Alcohol-induced facial dysmorphology in C57BL/6 mouse models of fetal alcohol spectrum disorder. Alcohol **44:** 659-671.

Armstrong, E. M., and E. L. Abel, 2000 Fetal alcohol syndrome: the origins of a moral panic. Alcohol Alcohol **35:** 276-282.

Arron, J. R., M. M. Winslow, A. Polleri, C. P. Chang, H. Wu *et al.*, 2006 NFAT dysregulation by increased dosage of DSCR1 and DYRK1A on chromosome 21. Nature **441:** 595-600.

Asagiri, M., K. Sato, T. Usami, S. Ochi, H. Nishina *et al.*, 2005 Autoamplification of NFATc1 expression determines its essential role in bone homeostasis. J Exp Med **202:** 1261-1269.

Awan, A., M. Bernstein, T. Hamasaki and P. Satir, 2004a Cloning and characterization of Kin5, a novel Tetrahymena ciliary kinesin II. Cell Motil Cytoskeleton **58:** 1-9.

Awan, A. K., D. A. Macafee and R. I. Hall, 2004b Intestinal obstruction in an adult with Down's syndrome. J R Soc Med **97:** 334-335.

Berend, S. A., S. L. Page, W. Atkinson, C. McCaskill, N. E. Lamb *et al.*, 2003 Obligate short-arm exchange in de novo Robertsonian translocation formation influences placement of crossovers in chromosome 21 nondisjunction. Am J Hum Genet **72:** 488-495.Berto, G., P. Camera, C. Fusco, S. Imarisio, C. Ambrogio *et al.*, 2007 The Down syndrome critical region protein TTC3 inhibits neuronal differentiation via RhoA and Citron kinase. J Cell Sci **120:** 1859-1867.

Bianchi, P., E. Ciani, S. Guidi, S. Trazzi, D. Felice *et al.*, 2010 Early pharmacotherapy restores neurogenesis and cognitive performance in the Ts65Dn mouse model for Down syndrome. J Neurosci **30:** 8769-8779.

Birger, Y., and S. Izraeli, 2012 DYRK1A in Down syndrome: an oncogene or tumor suppressor? J Clin Invest **122:** 807-810.

Blazek, J. D., A. Gaddy, R. Meyer, R. J. Roper and J. Li, 2011 Disruption of bone development and homeostasis by trisomy in Ts65Dn Down syndrome mice. Bone **48:** 275-280.

Bloemers, B. L., L. Bont, R. A. de Weger, S. A. Otto, J. A. Borghans *et al.*, 2011 Decreased thymic output accounts for decreased naive T cell numbers in children with Down syndrome. J Immunol **186:** 4500-4507.

Branchi, I., Z. Bichler, L. Minghetti, J. M. Delabar, F. Malchiodi-Albedi *et al.*, 2004 Transgenic mouse in vivo library of human Down syndrome critical region 1: association between DYRK1A overexpression, brain development abnormalities, and cell cycle protein alteration. J Neuropathol Exp Neurol **63:** 429-440.

Burd, L., E. Deal, R. Rios, E. Adickes, J. Wynne *et al.*, 2007 Congenital heart defects and fetal alcohol spectrum disorders. Congenit Heart Dis **2:** 250-255.

Burgio, G. R., A. Lanzavecchia, R. Maccario, A. Vitiello, A. Plebani *et al.*, 1978 Immunodeficiency in Down's syndrome: T-lymphocyte subset imbalance in trisomic children. Clin Exp Immunol **33:** 298-301.

Caley, L. M., C. Kramer and L. K. Robinson, 2005 Fetal alcohol spectrum disorder. J Sch Nurs **21:** 139-146.

Cartwright, M. M., and S. M. Smith, 1995 Increased cell death and reduced neural crest cell numbers in ethanol-exposed embryos: partial basis for the fetal alcohol syndrome phenotype. Alcohol Clin Exp Res **19:** 378-386.

Cebolla, A. M., G. Cheron, R. Hourez, B. Bearzatto, B. Dan *et al.*, 2009 Effects of maternal alcohol consumption during breastfeeding on motor and cerebellar Purkinje cells behavior in mice. Neurosci Lett **455:** 4-7.

Chakrabarti, L., T. K. Best, N. P. Cramer, R. S. Carney, J. T. Isaac *et al.*, 2010 Olig1 and Olig2 triplication causes developmental brain defects in Down syndrome. Nat Neurosci **13:** 927-934.

Chakrabarti, L., Z. Galdzicki and T. F. Haydar, 2007 Defects in embryonic neurogenesis and initial synapse formation in the forebrain of the Ts65Dn mouse model of Down syndrome. J Neurosci **27:** 11483-11495.

Chen, S. Y., D. B. Dehart and K. K. Sulik, 2004 Protection from ethanol-induced limb malformations by the superoxide dismutase/catalase mimetic, EUK-134. FASEB J **18:** 1234-1236.

Chen, Y., N. C. Ozturk, L. Ni, C. Goodlett and F. C. Zhou, 2011 Strain differences in developmental vulnerability to alcohol exposure via embryo culture in mice. Alcohol Clin Exp Res **35:** 1293-1304.

Coles, C. D., M. E. Lynch, J. A. Kable, K. C. Johnson and F. C. Goldstein, 2010 Verbal and nonverbal memory in adults prenatally exposed to alcohol. Alcohol Clin Exp Res **34:** 897-906.

Deitz, S. L., and R. J. Roper, 2011 Trisomic and Allelic Differences Influence Phenotypic Variability During Development of Down Syndrome Mice. Genetics **189:** 1487-1495.

Dunty, W. C., Jr., R. M. Zucker and K. K. Sulik, 2002 Hindbrain and cranial nerve dysmorphogenesis result from acute maternal ethanol administration. Dev Neurosci **24:** 328-342.

Elliott, E. J., J. Payne, A. Morris, E. Haan and C. Bower, 2008 Fetal alcohol syndrome: a prospective national surveillance study. Arch Dis Child **93:** 732-737.

Enomoto, A., H. Murakami, N. Asai, N. Morone, T. Watanabe *et al.*, 2005 Akt/PKB regulates actin organization and cell motility via Girdin/APE. Dev Cell **9:** 389-402.

Epstein, C. J., 2001 Down syndrome (trisomy 21), pp. 1223-1256 in *The Metabolic and Molecular Bases of Inherited Disease*, edited by A. L. B. C.R. Scriver, W.S. Sly, and D. Valle. McGraw-Hill, New York.

Epstein, C. J., 2006 Down's syndrome: critical genes in a critical region. Nature **441:** 582-583.

Ermak, G., T. E. Morgan and K. J. Davies, 2001 Chronic overexpression of the calcineurin inhibitory gene DSCR1 (Adapt78) is associated with Alzheimer's disease. J Biol Chem **276:** 38787-38794.

Farkas, L. G., M. J. Katic and C. R. Forrest, 2001 Surface anatomy of the face in Down's syndrome: anthropometric proportion indices in the craniofacial regions. J Craniofac Surg **12:** 519-524; discussion 525-516.

Ferrario, V. F., C. Dellavia, G. Zanotti and C. Sforza, 2004 Soft tissue facial anthropometry in Down syndrome subjects. J Craniofac Surg **15:** 528-532.

Ferrer, I., and E. Galofre, 1987 Dendritic spine anomalies in fetal alcohol syndrome. Neuropediatrics **18:** 161-163.

Fidler, D. J., and L. Nadel, 2007 Education and children with Down syndrome: neuroscience, development, and intervention. Ment Retard Dev Disabil Res Rev **13:** 262-271.

Flentke, G. R., A. Garic, E. Amberger, M. Hernandez and S. M. Smith, 2011 Calcium-mediated repression of beta-catenin and its transcriptional signaling mediates neural crest cell death in an avian model of fetal alcohol syndrome. Birth Defects Res A Clin Mol Teratol **91:** 591-602.

Florea, B. I., M. Verdoes, N. Li, W. A. van der Linden, P. P. Geurink *et al.*, 2010 Activity-based profiling reveals reactivity of the murine thymoproteasome-specific subunit beta5t. Chem Biol **17:** 795-801.

Foltran, F., D. Gregori, L. Franchin, E. Verduci and M. Giovannini, 2011 Effect of alcohol consumption in prenatal life, childhood, and adolescence on child development. Nutr Rev **69:** 642-659.

Fromigue, O., E. Hay, A. Barbara and P. J. Marie, 2010 Essential role of nuclear factor of activated T cells (NFAT)-mediated Wnt signaling in osteoblast differentiation induced by strontium ranelate. J Biol Chem **285:** 25251-25258.

Fuentes, J. J., L. Genesca, T. J. Kingsbury, K. W. Cunningham, M. Perez-Riba *et al.*, 2000 DSCR1, overexpressed in Down syndrome, is an inhibitor of calcineurin-mediated signaling pathways. Hum Mol Genet **9:** 1681-1690.

Gardiner, K., A. Fortna, L. Bechtel and M. T. Davisson, 2003 Mouse models of Down syndrome: how useful can they be? Comparison of the gene content of human chromosome 21 with orthologous mouse genomic regions. Gene **318:** 137-147.

Garic-Stankovic, A., M. R. Hernandez, P. J. Chiang, K. A. Debelak-Kragtorp, G. R. Flentke *et al.*, 2005 Ethanol triggers neural crest apoptosis through the selective activation of a pertussis toxin-sensitive G protein and a phospholipase Cbeta-dependent Ca2+ transient. Alcohol Clin Exp Res **29:** 1237-1246.

George, E. K., M. L. Mearin, J. Bouquet, B. M. von Blomberg, S. O. Stapel *et al.*, 1996 High frequency of celiac disease in Down syndrome. J Pediatr **128:** 555-557.

Gonzalez-Aguero, A., G. Vicente-Rodriguez, L. A. Moreno and J. A. Casajus, 2011 Bone mass in male and female children and adolescents with Down syndrome. Osteoporos Int **22:** 2151-2157.

Green, M. L., A. V. Singh, Y. Zhang, K. A. Nemeth, K. K. Sulik *et al.*, 2007 Reprogramming of genetic networks during initiation of the Fetal Alcohol Syndrome. Dev Dyn **236:** 613-631.

Gressens, P., M. Lammens, J. J. Picard and P. Evrard, 1992 Ethanol-induced disturbances of gliogenesis and neuronogenesis in the developing murine brain: an in vitro and in vivo immunohistochemical and ultrastructural study. Alcohol Alcohol **27:** 219-226.

Gupta, R., R. D. Thomas, V. Sreenivas, S. Walter and J. M. Puliyel, 2001 Ultrasonographic femur-tibial length ratio: a marker of Down syndrome from the late second trimester. Am J Perinatol **18:** 217-224.

Han, F., H. Yu, J. Zhang, C. Tian, C. Schmidt *et al.*, 2009 Otitis media in a mouse model for Down syndrome. Int J Exp Pathol **90:** 480-488.

Hans, P. S., R. England, S. Prowse, E. Young and P. Z. Sheehan, 2010 UK and Ireland experience of cochlear implants in children with Down syndrome. Int J Pediatr Otorhinolaryngol **74:** 260-264.

Hard, M. L., M. Abdolell, B. H. Robinson and G. Koren, 2005 Gene-expression analysis after alcohol exposure in the developing mouse. J Lab Clin Med **145:** 47-54.

Harris, C. D., G. Ermak and K. J. Davies, 2005 Multiple roles of the DSCR1 (Adapt78 or RCAN1) gene and its protein product calcipressin 1 (or RCAN1) in disease. Cell Mol Life Sci **62:** 2477-2486.

Hassold, T., and S. Sherman, 2000 Down syndrome: genetic recombination and the origin of the extra chromosome 21. Clin Genet **57:** 95-100.

Haydar, T. F., R. S. Nowakowski, P. J. Yarowsky and B. K. Krueger, 2000 Role of founder cell deficit and delayed neuronogenesis in microencephaly of the trisomy 16 mouse. J Neurosci **20:** 4156-4164.

Helguera, P., A. Pelsman, G. Pigino, E. Wolvetang, E. Head *et al.*, 2005 ets-2 promotes the activation of a mitochondrial death pathway in Down's syndrome neurons. J Neurosci **25:** 2295-2303.

Hofer, R., and L. Burd, 2009 Review of published studies of kidney, liver, and gastrointestinal birth defects in fetal alcohol spectrum disorders. Birth Defects Res A Clin Mol Teratol **85:** 179-183.

Huang, W. C., and C. C. Chen, 2005 Akt phosphorylation of p300 at Ser-1834 is essential for its histone acetyltransferase and transcriptional activity. Mol Cell Biol **25:** 6592-6602.

Ieraci, A., and D. G. Herrera, 2007 Single alcohol exposure in early life damages hippocampal stem/progenitor cells and reduces adult neurogenesis. Neurobiol Dis **26:** 597-605.

Incerti, M., J. Vink, R. Roberson, L. Wood, D. Abebe *et al.*, 2010 Reversal of alcohol-induced learning deficits in the young adult in a model of fetal alcohol syndrome. Obstet Gynecol **115:** 350-356.

Jacobson, S. W., J. L. Jacobson, M. E. Stanton, E. M. Meintjes and C. D. Molteno, 2011 Biobehavioral markers of adverse effect in fetal alcohol spectrum disorders. Neuropsychol Rev **21:** 148-166.

Jones, E. L., D. Aarsland, E. Londos and C. Ballard, 2012 A Pilot Study Examining Associations between DYRK1A and alpha-Synuclein Dementias. Neurodegener Dis.**10**: 229-31

Jones, K. L., and D. W. Smith, 1973 Recognition of the fetal alcohol syndrome in early infancy. Lancet **302:** 999-1001.

Kasahara, M., T. Suzuki and L. D. Pasquier, 2004 On the origins of the adaptive immune system: novel insights from invertebrates and cold-blooded vertebrates. Trends Immunol **25:** 105-111.

Khisti, R. T., J. Wolstenholme, K. L. Shelton and M. F. Miles, 2006 Characterization of the ethanol-deprivation effect in substrains of C57BL/6 mice. Alcohol **40:** 119-126.

Kim, S. S., and S. R. Seo, 2011 The regulator of calcineurin 1 (RCAN1/DSCR1) activates the cAMP response element-binding protein (CREB) pathway. J Biol Chem **286:** 37841-37848.

Kupferman, J. C., C. M. Druschel and G. S. Kupchik, 2009 Increased prevalence of renal and urinary tract anomalies in children with Down syndrome. Pediatrics **124:** e615-621.

Kurt, M. A., D. C. Davies, M. Kidd, M. Dierssen and J. Florez, 2000 Synaptic deficit in the temporal cortex of partial trisomy 16 (Ts65Dn) mice. Brain Res **858:** 191-197.

Kvigne, V. L., G. R. Leonardson, M. Neff-Smith, E. Brock, J. Borzelleca *et al.*, 2004 Characteristics of children who have full or incomplete fetal alcohol syndrome. J Pediatr **145:** 635-640.

Lee, Y., J. Ha, H. J. Kim, Y. S. Kim, E. J. Chang *et al.*, 2009 Negative feedback Inhibition of NFATc1 by DYRK1A regulates bone homeostasis. J Biol Chem **284:** 33343-33351.

Lindhurst, M. J., J. C. Sapp, J. K. Teer, J. J. Johnston, E. M. Finn *et al.*, 2011 A mosaic activating mutation in AKT1 associated with the Proteus syndrome. N Engl J Med **365:** 611-619.

Liu, Y., Y. Balaraman, G. Wang, K. P. Nephew and F. C. Zhou, 2009 Alcohol exposure alters DNA methylation profiles in mouse embryos at early neurulation. Epigenetics **4:** 500-511.

Lloret, A., M. C. Badia, E. Giraldo, G. Ermak, M. D. Alonso *et al.*, 2011 Amyloid-beta toxicity and tau hyperphosphorylation are linked via RCAN1 in Alzheimer's disease. J Alzheimers Dis **27:** 701-709.

Lomoio, S., E. Scherini and D. Necchi, 2009 Beta-amyloid overload does not directly correlate with SAPK/JNK activation and tau protein phosphorylation in the cerebellar cortex of Ts65Dn mice. Brain Res **1297:** 198-206.

Lorenzi, H., N. Duvall, S. M. Cherry, R. H. Reeves and R. J. Roper, 2010 PCR prescreen for genotyping the Ts65Dn mouse model of Down syndrome. Biotechniques **48:** 35-38.

Lu, J., G. Esposito, C. Scuderi, L. Steardo, L. C. Delli-Bovi *et al.*, 2011 S100B and APP promote a gliocentric shift and impaired neurogenesis in Down syndrome neural progenitors. PLoS One **6:** e22126.

Meintjes, E. M., J. L. Jacobson, C. D. Molteno, J. C. Gatenby, C. Warton *et al.*, 2010 An FMRI study of number processing in children with fetal alcohol syndrome. Alcohol Clin Exp Res **34:** 1450-1464.

Moller, R. S., S. Kubart, M. Hoeltzenbein, B. Heye, I. Vogel *et al.*, 2008 Truncation of the Down syndrome candidate gene DYRK1A in two unrelated patients with microcephaly. Am J Hum Genet **82:** 1165-1170.

Moore, C. S., J. S. Lee, B. Birren, G. Stetten, L. L. Baxter *et al.*, 1999 Integration of cytogenetic with recombinational and physical maps of mouse chromosome 16. Genomics **59:** 1-5.

Moore, E. S., R. E. Ward, P. L. Jamison, C. A. Morris, P. I. Bader *et al.*, 2002 New perspectives on the face in fetal alcohol syndrome: what anthropometry tells us. Am J Med Genet **109:** 249-260.

Moore, E. S., R. E. Ward, L. F. Wetherill, J. L. Rogers, I. Autti-Ramo *et al.*, 2007 Unique facial features distinguish fetal alcohol syndrome patients and controls in diverse ethnic populations. Alcohol Clin Exp Res **31:** 1707-1713.

Murata, S., K. Sasaki, T. Kishimoto, S. Niwa, H. Hayashi *et al.*, 2007 Regulation of CD8+ T cell development by thymus-specific proteasomes. Science **316:** 1349-1353.

Murata, S., Y. Takahama and K. Tanaka, 2008 Thymoproteasome: probable role in generating positively selecting peptides. Curr Opin Immunol **20:** 192-196.

Myrelid, A., J. Gustafsson, B. Ollars and G. Anneren, 2002 Growth charts for Down's syndrome from birth to 18 years of age. Arch Dis Child **87:** 97-103.

Norman, A. L., N. Crocker, S. N. Mattson and E. P. Riley, 2009 Neuroimaging and fetal alcohol spectrum disorders. Dev Disabil Res Rev **15:** 209-217.

O'Leary-Moore, S. K., S. E. Parnell, E. A. Godin, D. B. Dehart, J. J. Ament *et al.*, 2010 Magnetic resonance microscopy-based analyses of the brains of normal and ethanol-exposed fetal mice. Birth Defects Res A Clin Mol Teratol.

Ogawa, T., M. Kuwagata, J. Ruiz and F. C. Zhou, 2005 Differential teratogenic effect of alcohol on embryonic development between C57BL/6 and DBA/2 mice: a new view. Alcohol Clin Exp Res **29:** 855-863.

Park, J., Y. Oh and K. C. Chung, 2009a Two key genes closely implicated with the neuropathological characteristics in Down syndrome: DYRK1A and RCAN1. BMB Rep **42:** 6-15.

Park, J., W. J. Song and K. C. Chung, 2009b Function and regulation of Dyrk1A: towards understanding Down syndrome. Cell Mol Life Sci **66:** 3235-3240.

Park, J., E. J. Yang, J. H. Yoon and K. C. Chung, 2007 Dyrk1A overexpression in immortalized hippocampal cells produces the neuropathological features of Down syndrome. Mol Cell Neurosci **36:** 270-279.

Patra, A. K., S. Y. Na and U. Bommhardt, 2004 Active protein kinase B regulates TCR responsiveness by modulating cytoplasmic-nuclear localization of NFAT and NF-kappa B proteins. J Immunol **172:** 4812-4820.

Peng, X. D., P. Z. Xu, M. L. Chen, A. Hahn-Windgassen, J. Skeen *et al.*, 2003 Dwarfism, impaired skin development, skeletal muscle atrophy, delayed bone development, and impeded adipogenesis in mice lacking Akt1 and Akt2. Genes Dev **17:** 1352-1365.

Ram, G., and J. Chinen, 2011 Infections and immunodeficiency in Down syndrome. Clin Exp Immunol **164:** 9-16.

Reinholdt, L. G., Y. Ding, G. T. Gilbert, A. Czechanski, J. P. Solzak *et al.*, 2011 Molecular characterization of the translocation breakpoints in the Down syndrome mouse model Ts65Dn. Mamm Genome **22:** 685-691.

Resta, O., M. P. Barbaro, T. Giliberti, G. Caratozzolo, M. G. Cagnazzo *et al.*, 2003 Sleep related breathing disorders in adults with Down syndrome. Downs Syndr Res Pract **8:** 115-119.

Richtsmeier, J. T., L. L. Baxter and R. H. Reeves, 2000 Parallels of craniofacial maldevelopment in Down syndrome and Ts65Dn mice. Dev Dyn **217:** 137-145.

Richtsmeier, J. T., and V. B. Deleon, 2009 Morphological integration of the skull in craniofacial anomalies. Orthod Craniofac Res **12:** 149-158.

Riley, E. P., M. A. Infante and K. R. Warren, 2011 Fetal alcohol spectrum disorders: an overview. Neuropsychol Rev **21:** 73-80.

Roberson, R., I. Cameroni, L. Toso, D. Abebe, S. Bissel *et al.*, 2009 Alterations in phosphorylated cyclic adenosine monophosphate response element of binding protein activity: a pathway for fetal alcohol syndrome-related neurotoxicity. Am J Obstet Gynecol **200:** 193 e191-195.

Roper, R. J., J. F. VanHorn, C. C. Cain and R. H. Reeves, 2009 A neural crest deficit in Down syndrome mice is associated with deficient mitotic response to Sonic hedgehog. Mech Dev **126:** 212-219.

Ryoo, S. R., H. J. Cho, H. W. Lee, H. K. Jeong, C. Radnaabazar *et al.*, 2008 Dual-specificity tyrosine(Y)-phosphorylation regulated kinase 1A-mediated phosphorylation of amyloid precursor protein: evidence for a functional link between Down syndrome and Alzheimer's disease. J Neurochem **104:** 1333-1344.

Santagati, F., and F. M. Rijli, 2003 Cranial neural crest and the building of the vertebrate head. Nat Rev Neurosci **4:** 806-818.

Sari, Y., 2009 Activity-dependent neuroprotective protein-derived peptide, NAP, preventing alcohol-induced apoptosis in fetal brain of C57BL/6 mouse. Neuroscience **158:** 1426-1435.

Sasaki, K., J. Hamazaki, M. Koike, Y. Hirano, M. Komatsu *et al.*, 2010 PAC1 gene knockout reveals an essential role of chaperone-mediated 20S proteasome biogenesis and latent 20S proteasomes in cellular homeostasis. Mol Cell Biol **30:** 3864-3874.

Schaefer, G. B., and D. Deere, 2011 Recognition, diagnosis and treatment of fetal alcohol syndrome. J Ark Med Soc **108:** 38-40.

Selikowitz, M., 1993 A five-year longitudinal study of thyroid function in children with Down syndrome. Dev Med Child Neurol **35:** 396-401.

Servais, L., R. Hourez, B. Bearzatto, D. Gall, S. N. Schiffmann *et al.*, 2007 Purkinje cell dysfunction and alteration of long-term synaptic plasticity in fetal alcohol syndrome. Proc Natl Acad Sci U S A **104:** 9858-9863.

Shiojima, I., and K. Walsh, 2002 Role of Akt signaling in vascular homeostasis and angiogenesis. Circ Res **90:** 1243-1250.

Snow, M. E., and K. Keiver, 2007 Prenatal ethanol exposure disrupts the histological stages of fetal bone development. Bone **41:** 181-187.

Spender, Q., A. Stein, J. Dennis, S. Reilly, E. Percy *et al.*, 1996 An exploration of feeding difficulties in children with Down syndrome. Dev Med Child Neurol **38:** 681-694.

Spohr, H. L., J. Willms and H. C. Steinhausen, 2007 Fetal alcohol spectrum disorders in young adulthood. J Pediatr **150:** 175-179, 179 e171.

Srivastava, R. K., C. Y. Sasaki, J. M. Hardwick and D. L. Longo, 1999 Bcl-2-mediated drug resistance: inhibition of apoptosis by blocking nuclear factor of activated T lymphocytes (NFAT)-induced Fas ligand transcription. J Exp Med **190:** 253-265.

Streissguth, A. P., F. L. Bookstein, H. M. Barr, P. D. Sampson, K. O'Malley *et al.*, 2004 Risk factors for adverse life outcomes in fetal alcohol syndrome and fetal alcohol effects. J Dev Behav Pediatr **25:** 228-238.

Su, B., K. A. Debelak, L. L. Tessmer, M. M. Cartwright and S. M. Smith, 2001 Genetic influences on craniofacial outcome in an avian model of prenatal alcohol exposure. Alcohol Clin Exp Res **25:** 60-69.

Suizu, F., Y. Hiramuki, F. Okumura, M. Matsuda, A. J. Okumura *et al.*, 2009 The E3 ligase TTC3 facilitates ubiquitination and degradation of phosphorylated Akt. Dev Cell **17:** 800-810.

Sulik, K. K., 2005 Genesis of alcohol-induced craniofacial dysmorphism. Exp Biol Med (Maywood) **230:** 366-375.

Sun, X., Y. Wu, B. Chen, Z. Zhang, W. Zhou *et al.*, 2011 Regulator of calcineurin 1 (RCAN1) facilitates neuronal apoptosis through caspase-3 activation. J Biol Chem **286:** 9049-9062.

Unterberger, U., G. Lubec, M. Dierssen, G. Stoltenburg-Didinger, J. C. Farreras *et al.*, 2003 The cerebral cortex in fetal Down syndrome. J Neural Transm Suppl**:** 159-163.

Van Cleve, S. N., and W. I. Cohen, 2006 Part I: clinical practice guidelines for children with Down syndrome from birth to 12 years. J Pediatr Health Care **20:** 47-54.

Wang, G., and E. Bieberich, 2010 Prenatal alcohol exposure triggers ceramide-induced apoptosis in neural crest-derived tissues concurrent with defective cranial development. Cell Death Dis **1:** e46.

Wang, R., and M. G. Brattain, 2006 AKT can be activated in the nucleus. Cell Signal **18:** 1722-1731.

Wegiel, J., C. X. Gong and Y. W. Hwang, 2011a The role of DYRK1A in neurodegenerative diseases. FEBS J **278:** 236-245.

Wegiel, J., W. Kaczmarski, M. Barua, I. Kuchna, K. Nowicki *et al.*, 2011b Link between DYRK1A overexpression and several-fold enhancement of neurofibrillary degeneration with 3-repeat tau protein in Down syndrome. J Neuropathol Exp Neurol **70:** 36-50.

Weijerman, M. E., A. M. van Furth, M. D. van der Mooren, M. M. van Weissenbruch, L. Rammeloo *et al.*, 2010 Prevalence of congenital heart defects and persistent pulmonary hypertension of the neonate with Down syndrome. Eur J Pediatr **169:** 1195-1199.

Williams, A. D., C. H. Mjaatvedt and C. S. Moore, 2008 Characterization of the cardiac phenotype in neonatal Ts65Dn mice. Dev Dyn **237:** 426-435.

Wiseman, F. K., K. A. Alford, V. L. Tybulewicz and E. M. Fisher, 2009 Down syndrome--recent progress and future prospects. Hum Mol Genet **18:** R75-83.

Wyper, K. R., and C. R. Rasmussen, 2011 Language impairments in children with fetal alcohol spectrum disorders. J Popul Ther Clin Pharmacol **18:** e364-376.

Xu, J., J. E. Yeon, H. Chang, G. Tison, G. J. Chen *et al.*, 2003 Ethanol impairs insulin-stimulated neuronal survival in the developing brain: role of PTEN phosphatase. J Biol Chem **278:** 26929-26937.

Yabut, O., J. Domogauer and G. D'Arcangelo, 2010 Dyrk1A overexpression inhibits proliferation and induces premature neuronal differentiation of neural progenitor cells. J Neurosci **30:** 4004-4014.

TABLES

Table 1 Phenotypic Analysis of DS and FAS: A review of over 15 studies investigating craniofacial, structural, and cognitive traits in both humans and mouse models of DS and FAS. All studies show significant similarities between DS and FAS except one, the minimal front breadth in the mouse models

		Human		Mouse	
	Traits	**DS**	**FAS**	**DS**	**FAS**
Craniofacial Anthropometry	**Minimal Front Breadth**	Smaller(Allanson *et al.* 1993; Farkas *et al.* 2001)	Smaller(Moore *et al.* 2002; Moore *et al.* 2007)	Larger(Richtsmeier *et al.* 2000)	Smaller(Anthony *et al.* 2010a)
	Skull Base Breadth	Smaller(Allanson *et al.* 1993; Farkas *et al.* 2001)	Smaller(Moore *et al.* 2002; Moore *et al.* 2007)	Smaller(Richtsmeier *et al.* 2000)	Smaller(Anthony *et al.* 2010b)
	Upper & Lower Facial Width	Smaller(Allanson *et al.* 1993; Farkas *et al.* 2001)	Smaller(Moore *et al.* 2002; Moore *et al.* 2007)	Smaller	Smaller(Anthony *et al.* 2010b)
	Canthal Distances	Smaller(Allanson *et al.* 1993)	Smaller(Moore *et al.* 2002; Moore *et al.* 2007)	Smaller(Richtsmeier *et al.* 2000)	Smaller(Anthony *et al.* 2010b)
	Palpebral Fissure	Smaller(Farkas *et al.* 2001)	Smaller(Moore *et al.* 2002; Moore *et al.* 2007)	N/A	Smaller(Anthony *et al.* 2010b)
	Nasal	Smaller(Allanson *et al.* 1993; Farkas *et al.* 2001; Ferrario *et al.* 2004)	Smaller(Moore *et al.* 2002; Moore *et al.* 2007)	Smaller(Richtsmeier *et al.* 2000)	Smaller(Anthony *et al.* 2010b)
	Philtrum Length	Smaller(Farkas *et al.* 2001; Ferrario *et al.* 2004)	Smaller(Moore *et al.* 2002; Moore *et al.* 2007)	N/A	Larger(Anthony *et al.* 2010b)
	Facial Height	Smaller(Allanson *et al.* 1993; Farkas *et al.* 2001)	Smaller(Moore *et al.* 2007)	N/A	Smaller
	Facial Depth	Smaller(Allanson *et al.* 1993)	Smaller(Moore *et al.* 2002; Moore *et al.* 2007)	N/A	Smaller(Anthony *et al.* 2010b)
	Maxillary & Mandibular Arc	Smaller(Allanson *et al.* 1993)	Smaller(Moore *et al.* 2002; Moore *et al.* 2007)	Smaller*	N/A
	Head Circumfrence	Smaller(Allanson *et al.* 1993)	Smaller(Moore *et al.* 2002)	Smaller*	Smaller*
Brain	**Microcephaly**	Present(Moller *et al.* 2008)	Present(Elliott *et al.* 2008)	Present(Haydar *et al.* 2000)	Present(O'Leary-Moore *et al.* 2010)
	Cerebellum	Reduced(Fidler and Nadel 2007)	Reduced(Norman *et al.* 2009)	Purkinje Cells(Lomoio *et al.* 2009)	Purkinje cells(Cebolla *et al.* 2009; Servais *et al.* 2007)
	Hippocampus	Reduced(Fidler and Nadel 2007)	Reduced(Norman *et al.* 2009)	Dentate Gyrus(Bianchi *et al.* 2010)	Dentate Gyrus(Roberson *et al.* 2009)
	Cortex	Neuronal Impairment(Unterberger *et al.* 2003)	Neuronal Impairment(Ferrer and Galofre 1987; Meintjes *et al.* 2010)	Neuronal Impairment(Chakrabarti *et al.* 2007)	Neuronal Impairment(Incerti *et al.* 2010)
	Learning	Impaired(Fidler and Nadel 2007)	Impaired(Caley *et al.* 2005; Streissguth *et al.* 2004)	Impaired(Kurt *et al.* 2000)	Impaired(Ieraci and Herrera 2007)
	Memory	Impaired(Fidler and Nadel 2007)	Impaired(Coles *et al.* 2010)	Impaired(Kurt *et al.* 2000)	Impaired(Ieraci and Herrera 2007)
Other organ/ structure	**Heart**	Septal(Weijerman *et al.* 2010)	Septal(Burd *et al.* 2007)	Septal(Williams *et al.* 2008)	N/A
	Bone Development	Reduced(Gonzalez-Aguero *et al.* 2011)	Reduced(Snow and Keiver 2007)	Reduced(Blazek *et al.* 2010)	N/A
	Stature	Short(Myrelid *et al.* 2002)	Short(Spohr *et al.* 2007)	Short(Blazek *et al.* 2010)	N/A
	Limbs	Malformed(Gupta *et al.* 2001)	N/A	N/A	Malformed(Chen *et al.* 2004)
	Hearing	Loss(Hans *et al.* 2010)	Loss(Kvigne *et al.* 2004)	Loss(Han *et al.* 2009)	N/A
	Kidney	Displasia(Kupferman *et al.* 2009)	Displasia(Hofer and Burd 2009)	N/A	N/A
	GI tract	Pseudoobstruction(Awan *et al.* 2004a)	Pseudoobstruction(Hofer and Burd 2009)	N/A	N/A

Table 2 *Dyrk1a* and *Rcan1* Expression: Summary of qPCR analysis of both *Dyrk1a* and *Rcan1* expression in both DS and FAS mouse models. Note that the fold changes of these two cardinal genes are similarly expressed in the BA1

	Ts65Dn Dyrk1a	Ethanol Dyrk1a	Ts65Dn Rcan1	Ethanol Rcan1
BA1	0.644	0.701	1.255	1.963
Head	0.605	1.098	1.245	0.807
Body	0.675	1.377	1.015	1.126

Table 3 c-Caspase Expression: Ratio of apoptotic expression was analyzed in a previous study of ethanol treated embryos (CHEN *et al.* 2011) and was compared to Ts65Dn. The ratios both display significant increases when compared to their respective controls. Both models embryos were selected for similar somite age (24-28). Ts65Dn n=3, Ethanol treated n=4

Tissue	Ratio Trisomic:Euploid	Ratio Ethanol:Control
First Branchial Arch	2.63:1	5.47:1
Forebrain	2.67:1	3.29:1
Midbrain	1.51:1	2.52:1
Hindbrain	1.20:1	1.59:1

FIGURES

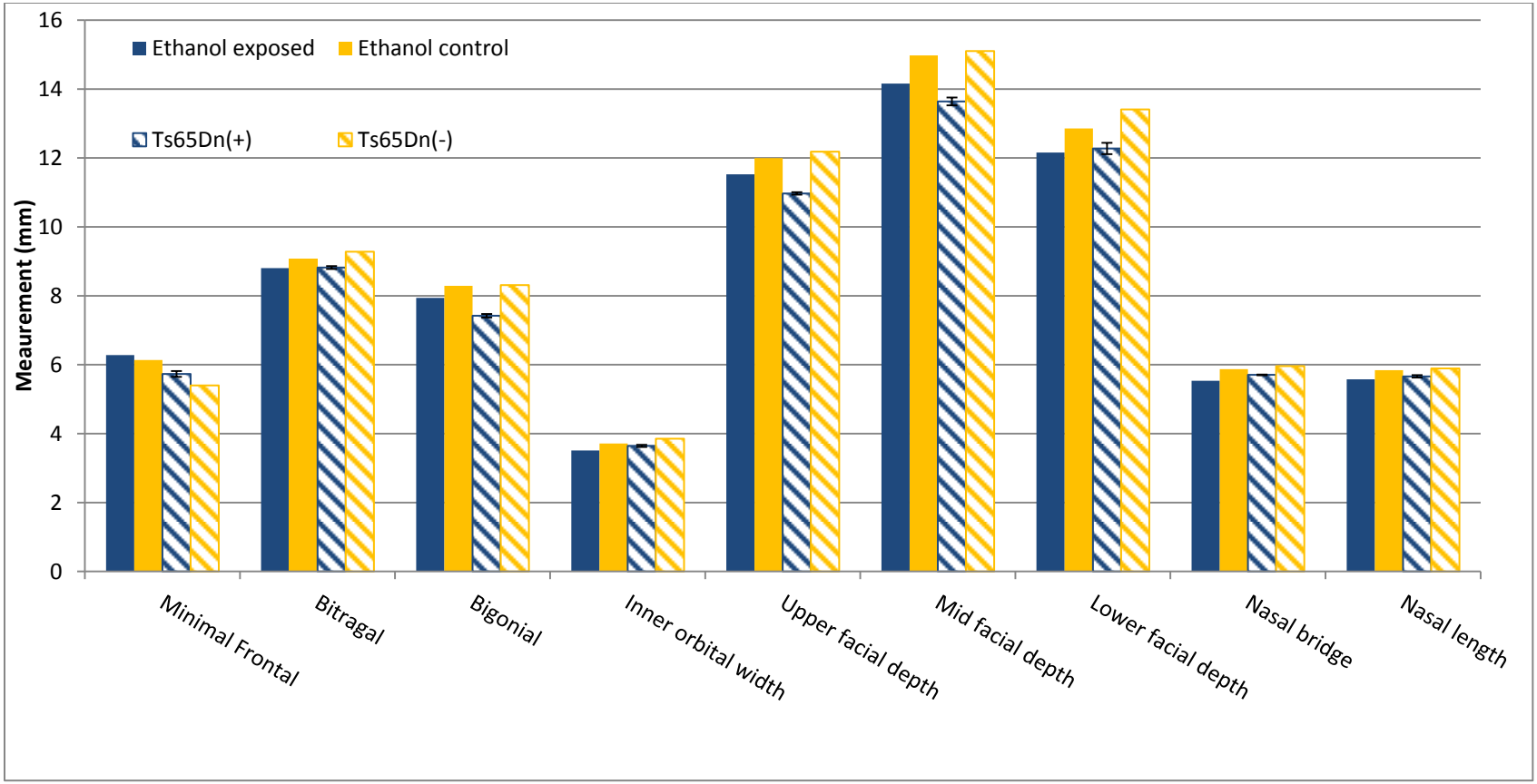

Figure 1 MicroCT analysis: These measurements are taken from Ts65Dn(+) and ethanol treated mice at P21. They are compared to controls of both models, Ts65Dn(-) and untreated C57BL/6 mice. The nine measurements are to show similar craniofacial abnormalities as seen in humans with DS and FAS

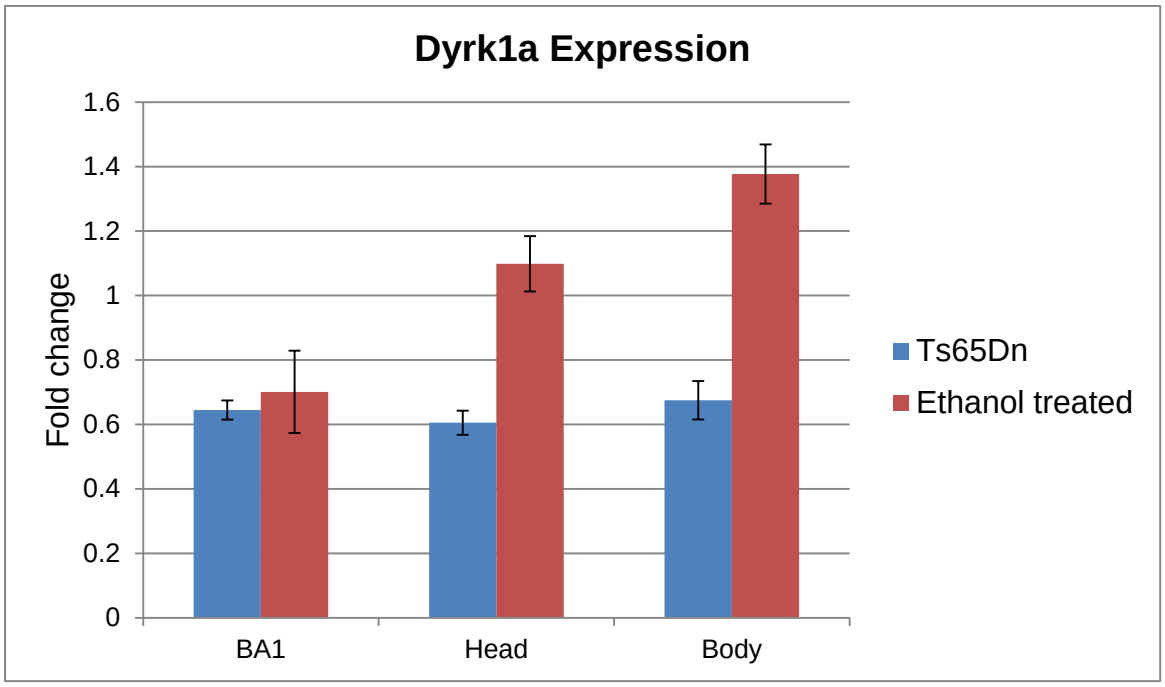

Figure 2 *Dyrk1a* Expression in DS and FAS Mouse Models: The qPCR analysis of *Dyrk1a* in Ts65Dn and ethanol treated embryos at E10 display dysregulation throughout. The BA1 however presents similar expression which is relevant to craniofacial deficits. Ts65Dn displays a more consistent expression throughout the tissues. The ethanol treated embryos present a less consistent expression having decreased expression in the BA1, slightly normal expression in the head, and over expression in the body. The error bars represent a standard error. All tissues from both DS and FAS models contained sample sizes of 5

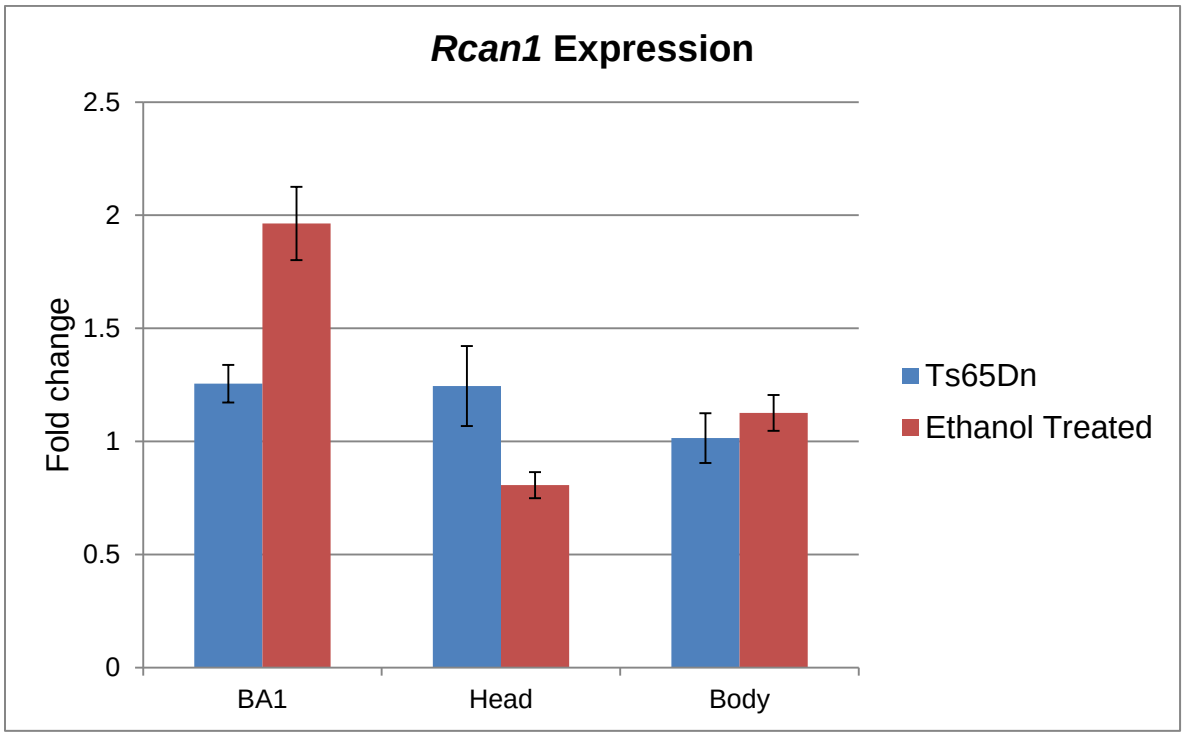

Figure 3 *Rcan1* Expression in DS and FAS Mouse Models: qPCR analysis of *Rcan1*, like *Dyrk1a*, also displays dysregulation throughout the embryo at E10 in both DS and FAS models. There is a similar increase in expression in the BA1, once again showing possible origins of similar craniofacial deficits. Error bars represent standard error. All tissues and models contain a sample size of 5

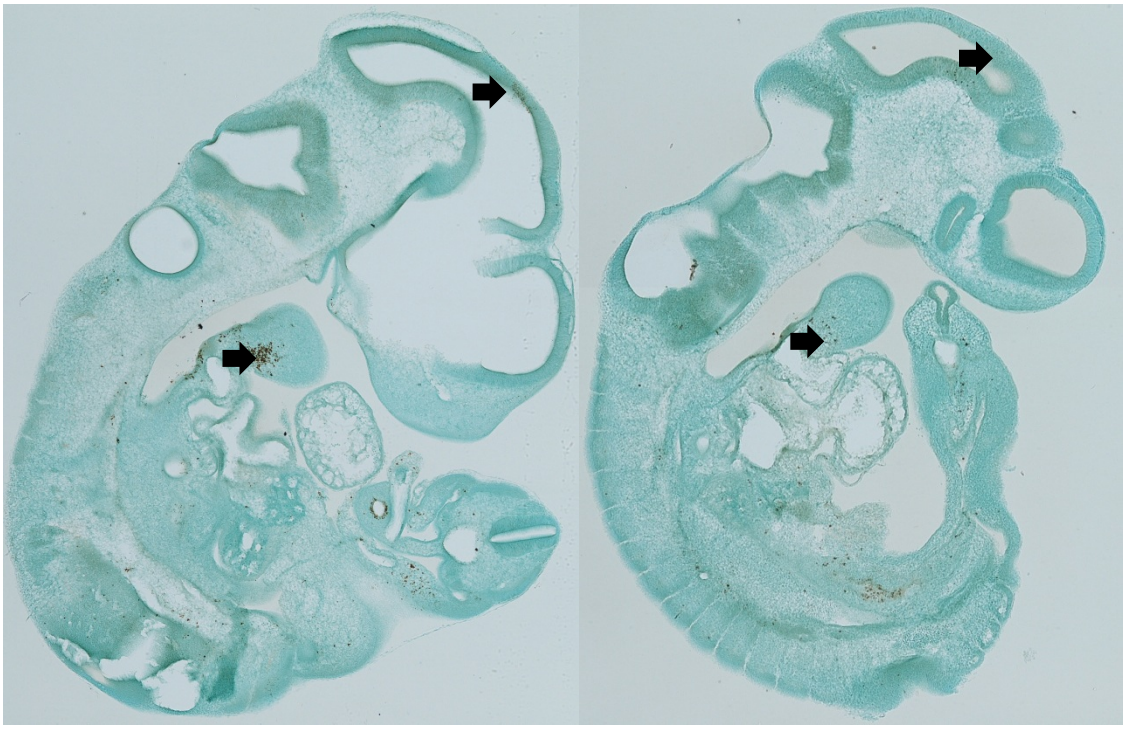

Figure 4 Immunohistochemistry analysis using Caspase 3: Two embryos, Trisomic (L) and Euploid (R), were stained for c-Caspase 3. A total of 3 comparisons, 3 trisomic and 3 euploid, were carried out. Arrows in this representation point to areas of significance including the BA1 and the midbrain

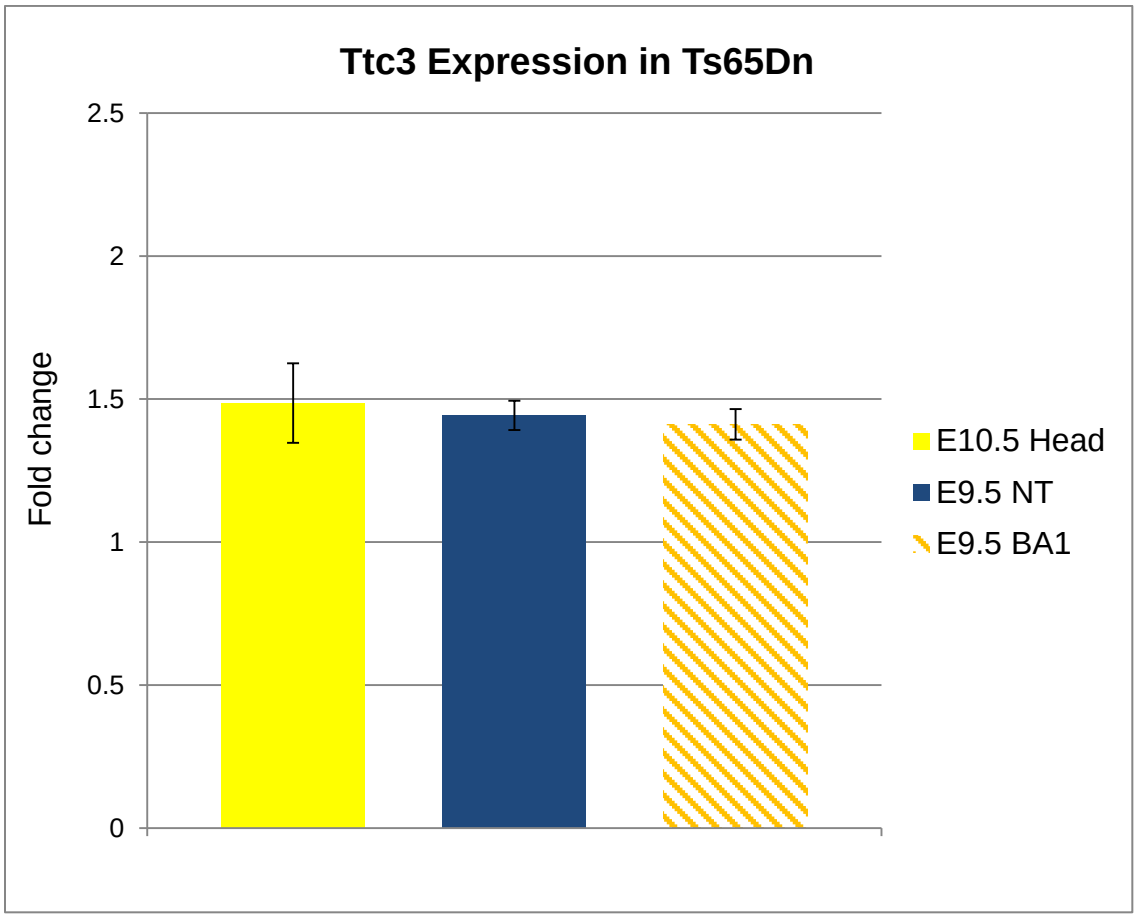

Figure 5 *Ttc3* Expression in Ts65Dn: *Ttc3* expression in three different tissues of Ts65Dn mice were analyzed using qPCR . All three tissues display an increase of approximately 1.5 fold over control embryos. Sample size for the head, NT, and BA1 is n=6, 4, and 5 respectively

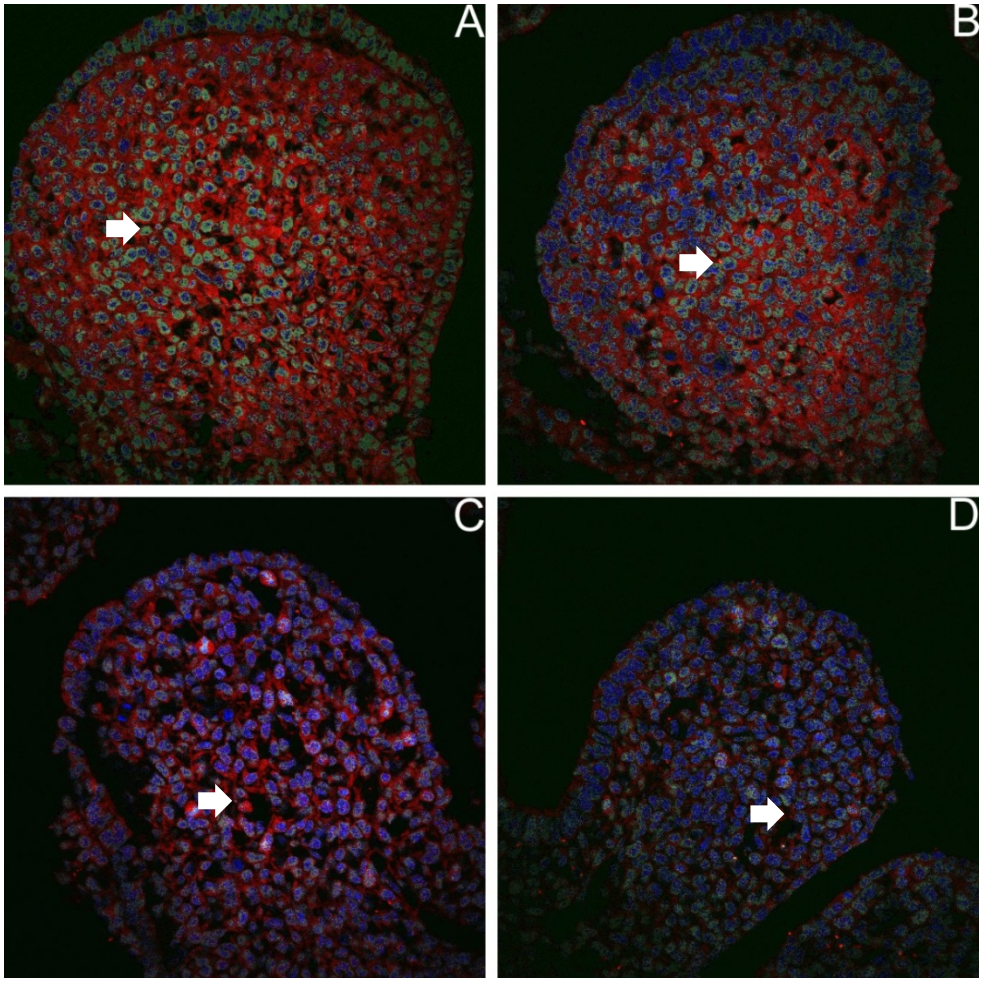

Figure 6 40X immunofluorescence of pAkt in the BA1 of Ts65Dn: In A and B is normal euploid expression of activated Akt. Red stain is pAkt, blue is DAPI nuclear staining, and green is the localization of both DAPI and pAkt showing activity in the nucleus. In C and D, Trisomic BA1s were stained and analyzed in the same fashion. There is a significant amount more of nuclear pAkt in euploid BA1 when compared to trisomic BA1. Arrows label cells within the BA1 that are indicative of the results found. Note that the euploid cells (A, B) contain much more pAkt within the nucleus than the trisomic cells (C, D) and that the organization and number of trisomic cells is much less

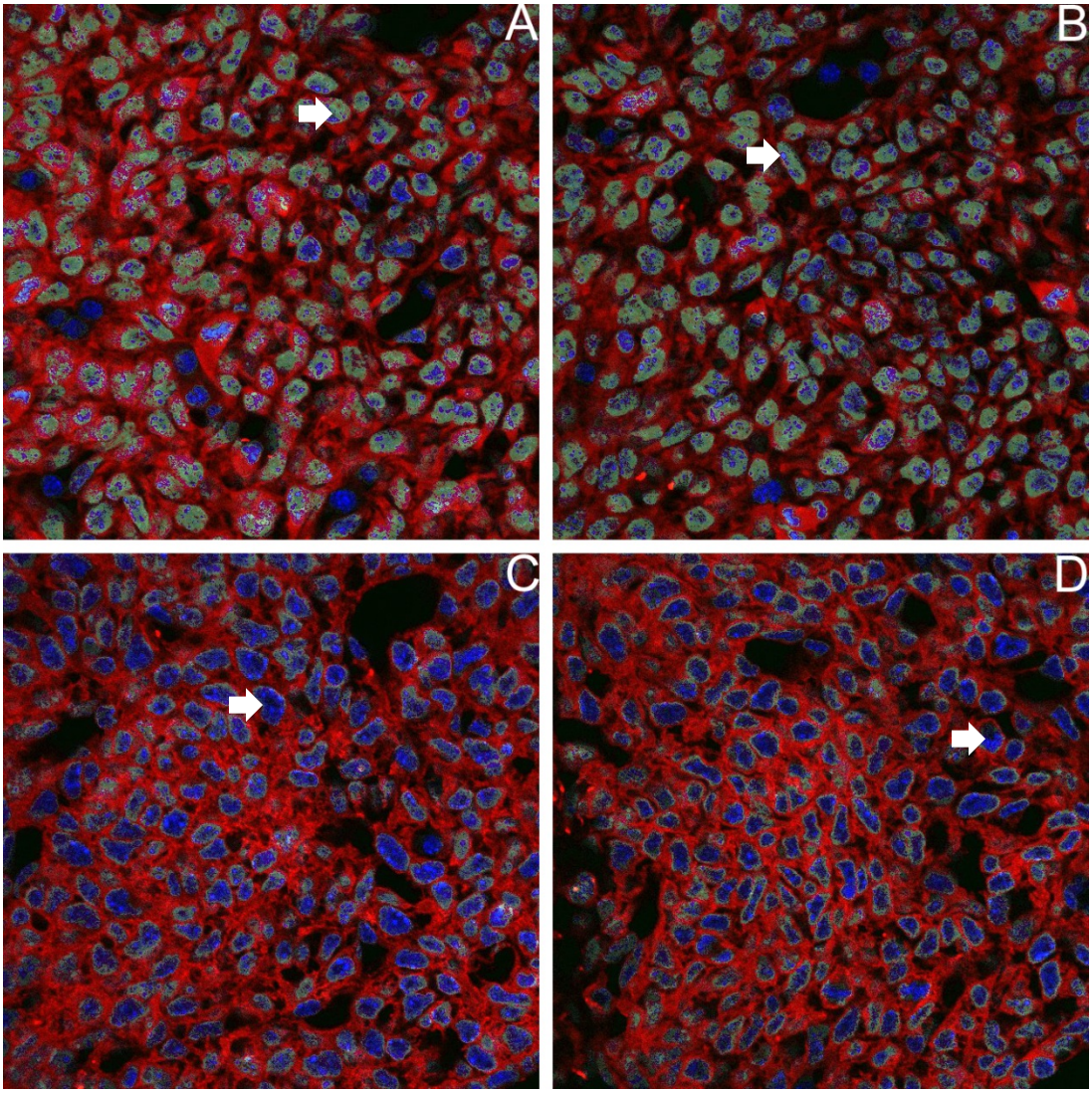

Figure 7 80x Immunofluorescence of pAkt in the BA1 in Ts65Dn: A closer view of euploid (A, B) and trisomic (C, D) cells show the difference more clearly

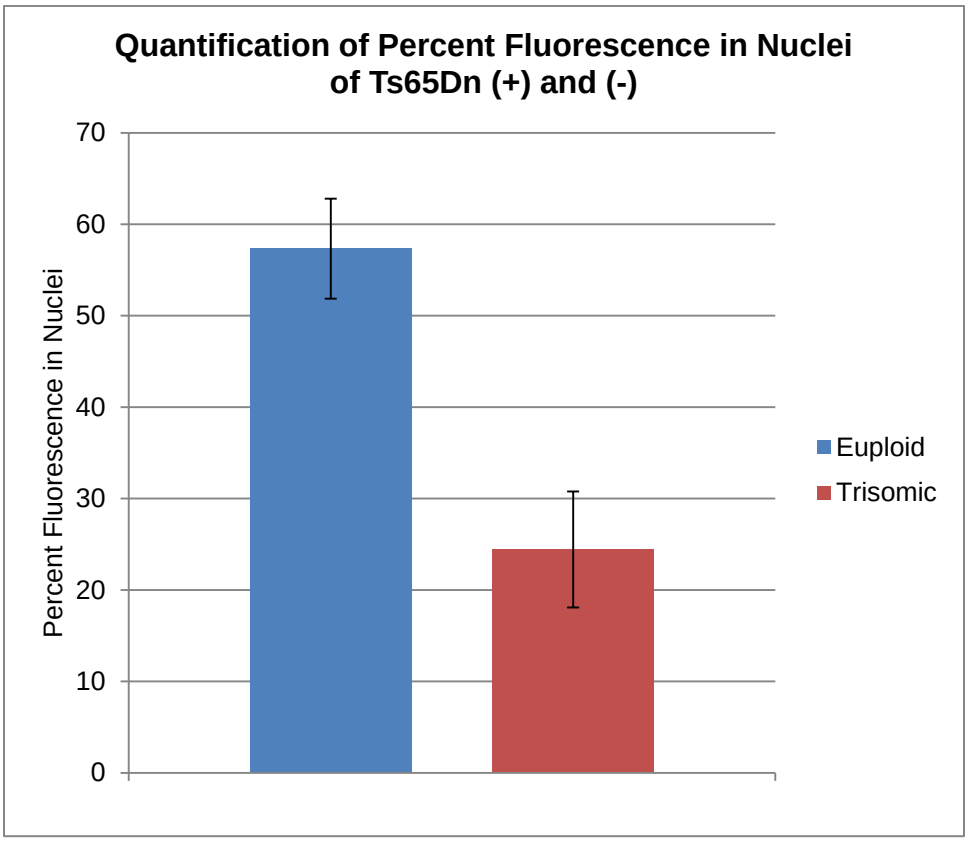

Figure 8 Immunofluorescence Analysis of pAkt expression in the nucleus: The quantification of overall percent of pAkt fluorescence in trisomic and euploid BA1 nuclei. Error bars indicate standard error. Sample size for euploid analysis was 3 different embryos and 14 sections. Trisomic analysis contained 4 total embryos and 13 sections. Fluorescence was analyzed using ImageJ

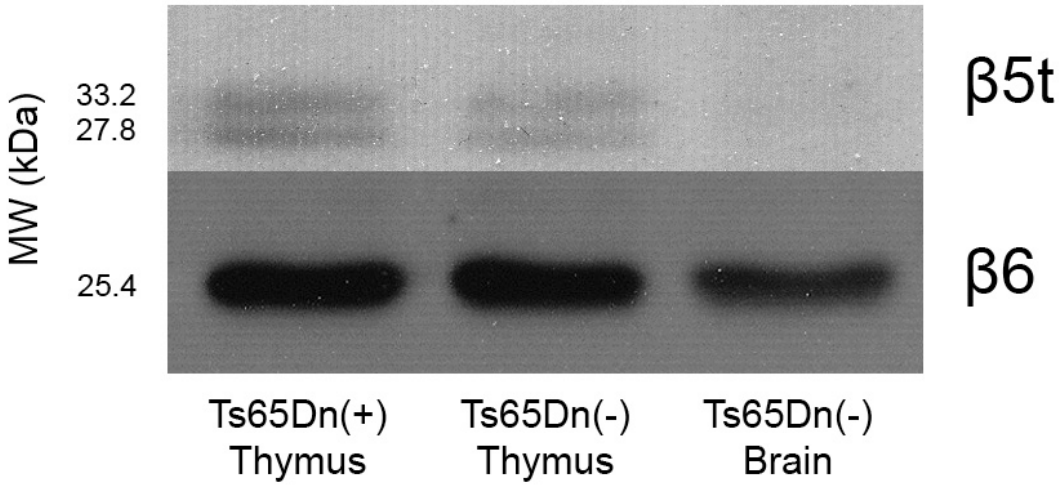

Figure 9 Proteasome Subunit Analysis on Ts65Dn Thymic Tissue: Western blot of proteins isolated from Ts65Dn trisomic and euploid thymus and brain. β5t and β6 showed no significant difference in expression between trisomic and euploid thymus. Ts65Dn(-) was used as both positive and negative control with β5t having no expression in the brain and β6 having a decreased expression compared to thymic tissue